Durable high early strength concrete via internal curing approach using saturated lightweight and recycled concrete aggregates

by

Faisal A. F. Qadri

B.S., An-Najah National University, 2016

A THESIS

submitted in partial fulfillment of the requirements for the degree

MASTER OF SCIENCE

Department of Civil Engineering
Carl R. Ice College of Engineering

KANSAS STATE UNIVERSITY
Manhattan, Kansas

2020

Approved by:

Major Professor
Dr. Christopher A. Jones

Copyright

Abstract

Environmental exposure is one of the primary causes of concrete pavement deterioration, specifically cyclic freezing and thawing, as is common in Kansas. Rehabilitation of deteriorated concrete pavement is a common pavement life-extension strategy, and a variety of rehabilitation techniques are often utilized depending on the level of pavement distress. Budgetary constraints, however, often dictate use of partial and full-depth patching methods to rehabilitate deteriorated concrete pavement rather than replace an entire road. For roadways with high traffic volume, patching is often done overnight within few hours. These repairs include removing the old concrete and preparing the location for new concrete, which must achieve at least 1,800 psi compressive strength 6 hours prior to opening to traffic to avoid compromising future durability. Current patches last less than 10 years despite a nominal 20-year service life.

This study utilized an internal curing technique to produce durable high early strength concrete for patching. Because desorbing water throughout the concrete matrix improves the microstructure and reduces porosity, lightweight aggregates and crushed concrete aggregates were each used to desorb water and provide internal curing. Tests were conducted to evaluate compressive strength, autogenous shrinkage, length change, and freezing and thawing related to mass change, length change, and relative dynamic modulus of elasticity (RDME). In contrast to ASTM C157, which only measures drying shrinkage after 14 days of curing, autogenous shrinkage of concrete was measured in this study. KTMR-22, developed by the Kansas Department of Transportation, was used to evaluate freeze-thaw durability of internally cured repair mixtures because this method subjects test specimens to a much harsher test regimen than ASTM C666. For example, KTMR-22 utilizes 660 cycles that simulate 20 years of exposure to 33 cycles of freezing and thawing compared to ASTM-666 exposure of only 300 cycles. Results showed that the mixture

made with lightweight aggregate and low cement content met all requirements for expansion and RDME. This mixture also had minimum autogenous shrinkage among all the mixtures.

Table of Contents

List of Figures viii
List of Tables x
Acknowledgements xi
Dedication xii
Chapter 1 - Introduction 1
1.1 Background 2
1.2 Problem Statement 3
1.3 Objective 3
Chapter 2 - Literature Review 5
2.1 Early Concrete Pavement Damage 5
2.2 Crack Development 5
2.2.1 Microstructure 5
2.2.2 Aggregate Size and Volume Fraction 7
2.2.3 Mechanical Loading and Freeze-Thaw Mechanisms 8
2.2.4 Joints and Sealants 9
2.3 High Early-Strength Concrete 11
2.4 Durability Practices 14
2.4.1 Supplementary Cementitious Material 14
2.4.2 Nano Particles 16
2.4.3 Engineering Cementitious Composites 18
2.5 Internal Curing 19
2.5.1 Proportioning 20
2.5.2 Strength and Elastic Modulus 23
2.5.2.1 Compressive Strength 23
2.5.2.2 Flexural Strength 24
2.5.2.3 Modulus of Elasticity 25
2.5.3 Shrinkage Mitigation 26
2.5.3.1 Plastic Shrinkage 26
2.5.3.2 Autogenous Shrinkage 28

2.5.3.3 Drying Shrinkage 30
2.5.4 Warping 32
2.5.5 Freezing and Thawing 32
2.5.6 Projects with Internally Cured Concrete 33
2.5.6.1 High Early-Strength ICC Off Ramp of I-635 in Mesquite, Texas 33
2.5.6.2 Dallas Intermodal Terminal 33
2.5.6.3 State Highway 121 North of Dallas, Texas 34
2.5.7 Internal Curing in Practice 34
2.6 Summary 34
Chapter 3 - Materials 36
3.1 Aggregates 36
3.1.1 Fine Aggregates 36
3.1.2 Coarse Aggregates 37
3.1.3 Lightweight Aggregates 38
3.1.4 Crushed Concrete Aggregates 40
3.2 Admixtures 41
3.2.1 Water Reducer 42
3.2.2 Air Entrainer 42
3.2.3 Accelerator 43
3.3 Cement 43
Chapter 4 - Methodology 45
4.1 Ingredient Selection and Proportions 45
4.2 Replacement 46
4.3 Small-Trial Mixtures 46
4.3.1 Slump Test 47
4.3.2 Air Content 48
4.4 Full-Batch Mixing 49
4.5 Tests and Standards 51
4.5.1 Compressive Strength 51
4.5.2 Autogenous Shrinkage 51
4.5.3 Drying Shrinkage 54

4.5.4 Freezing and Thawing 55
Chapter 5 - Results 57
5.1 Compressive Strength 57
5.2 Autogenous Shrinkage 58
5.3 Drying Shrinkage 59
5.4 Freezing and Thawing 60
Chapter 6 - Discussion 63
Chapter 7 - Conclusion 65
References 67

List of Figures

Figure 1-1: Prematurely Deteriorated Slabs in Garden City, Kansas 2
Figure 2-1: Schematic of Relation between Degree of Saturation and F/T Damage..... 10
Figure 2-2: Compressive Strength for CSA and CEM III Concretes at w/c 0.45 (Guan et al., 2017) 13
Figure 2-3: Shrinkage for CSA and CEM III Concretes at w/c 0.45 (Guan et al., 2017)..... 14
Figure 2-4: Water Absorption of Specimens (%) (Shekari & Razzaghi, 2011) 17
Figure 2-5: Chloride Penetration in Examined Specimens (Shekari & Razzaghi, 2011)..... 18
Figure 2-6: Desirable and Undesirable Aggregate Desorption Behavior (Castro, 2011)..... 22
Figure 2-7: Fitness Modulus Values and Volume of Protected Paste in Concrete with 30% Aggregate Replaced with Coarse Aggregate or Sand (Henkensiefken et al., 2009b) 23
Figure 2-8: Flexural Strength of UHPC with w/c and SAP (Justs et al., 2015)..... 25
Figure 2-9: Elastic Modulus of Sealed Specimens after IC (Golias, 2010)..... 26
Figure 2-10: Water-Filled LWA Exposed to Drying (Henkensiefken et al., 2010) 27
Figure 2-11: Probability Distribution of Crack Width Occurrences in Concrete with Replacement Volumes of Pre-wetted LWA (Henkensiefken et al., 2010)..... 28
Figure 2-12: Autogenous Deformation Measurements on Cement Mortars (Henkensiefken et al., 2009a) 29
Figure 2-13: Restrained Shrinkage Results for Mortars with Sealed Curing Conditions (Henkensiefken et al., 2009a) 30
Figure 2-14: Measured Deformation of Free Shrinkage Specimens with Unsealed Curing Conditions (Henkensiefken et al., 2009a)..... 31
Figure 2-15: Restrained Shrinkage Results for Mortars with Unsealed Curing Conditions. (Henkensiefken et al., 2009a) 31
Figure 3-1: Natural Sand-Fine Aggregate..... 36
Figure 3-2: Natural Gravel-Coarse Aggregate..... 38
Figure 3-3: Fine Lightweight Aggregates..... 39
Figure 3-4: CCA 41
Figure 4-1: Slump Test Apparatus..... 48
Figure 4-2: SAM Apparatus..... 49

Figure 4-3: Mud Hog Mixer 50
Figure 4-4: Autogenous Shrinkage Apparatus 53
Figure 4-5: Prisms Measuring Autogenous Shrinkage in Concrete 53
Figure 4-6: Length-Change Comparator (ASTM C157) 54
Figure 4-7: Scientemp F/T Machine 56
Figure 5-1: Compressive Strength Values for All Batches 57
Figure 5-2: Autogenous Shrinkage Measurements for All Batches 58
Figure 5-3: Drying Shrinkage Measurements for All Batches 59
Figure 5-4: Mass-Change Measurements for All Batches 60
Figure 5-5: Expansion Measurements for All Batches 61
Figure 5-6: RDME Measurements for All Batches 62

List of Tables

Table 2-1: Compressive Strength of RHA (Saraswathy & Song, 2007) 15
Table 2-2: Porosity of RHA (Saraswathy & Song, 2007) 15
Table 2-3: Chloride Diffusivity of RHA (Saraswathy & Song, 2007) 16
Table 2-4: Compressive Strength of Specimens after 28 Days (Shekari & Razzaghi, 2011) 17
Table 2-5: Distances Water Traveled from Surfaces of Internal Reservoirs (Bentz et al., 2007) 22
Table 2-6: Concrete Properties for NYSDOT Bridges (Streeter et al., 2012) 24
Table 2-7: Impact of IC Properties on High-Performance Concrete (Cusson & Margeson, 2010) 33
Table 3-1: Sieve Analysis for Fine Aggregates 37
Table 3-2: Sieve Analysis for Coarse Aggregates 38
Table 3-3: Sieve Analysis for LWA 40
Table 3-4: Sieve Analysis for CCA 41
Table 3-5: CEM III Chemical and Physical Properties 44
Table 4-1: Matrix of Mixtures 45
Table 4-2: Concrete Mix Designs 51

Acknowledgements

This study was supported by the Kansas Department of Transportation. A great deal of thanks to have this chance to do this project.

I would like to offer a special thanks to my advisor Dr. Christopher A. Jones for guiding me to produce this work and giving me as much knowledge as he can. He was always generous to give all of what I needed. He let me feel comfortable while I was in this program.

Also, I am thankful to the committee members, Professor Hayder A. Rasheed and Professor Mustaque Hossain, for taking the time to go through this thesis and judge me during the oral examination.

I do not forget to thank the heart of the laboratory, Benjamin Thurlow and Cody Delaney, for all the work they helped me to achieve and all the materials they provided.

I would also like to thank Trinity Lightweight for the generous donation of lightweight aggregates.

Dedication

I always say "*who does not thank people, does not thank God."* I would dedicate this work to my family and especially my parents, who supported me and encouraged me to go forward with my plans, who always saw and believed that I would be something big in the future. May God protect them. I offer a special thanks to my close friends for also supporting me while I had many obstacles prior coming to the United States and starting my graduate studies. I consider them brothers alike. I would like to specifically thank Helal Asfour, Feras Elsaid, Wasef Sayeh, Watheq Sayeh, Loai Bitawi, and Nayef Maqboul for everything they did to help me reach this moment and write this thesis.

Chapter 1 - Introduction

Concrete pavement is a primary component of the transportation infrastructure, making durability an essential element of infrastructure longevity worldwide. Based on the ASCE 2017 Infrastructure Report Card, $420 billion and $167 billion are needed to repair existing highways and highway system expansion in the United States, respectively (ASCE, 2017). Due to high costs associated with highway repairs, most states utilize infrastructure rehabilitation to extend the service life of a pavement and delay reconstruction. Selection of an effective rehabilitation strategy depends on the level of existing distress and available budget. The primary methods of rehabilitation are restoration, resurfacing, and reconstruction, which includes partial and full-depth repair patching. Distresses such as shattered slabs, longitudinal and horizontal full-depth cracks, and spalls require reconstruction.

Pavement repair is an economically efficient method to remediate deteriorated concrete pavement. In addition to standard specifications in section 833 of the Kansas Standards Specification for State Road and Bridge construction, the Kansas Department of Transportation (KDOT) has stipulated that concrete patches must achieve compressive or flexural strengths of at least 1,800 psi or 380 psi, respectively, prior to reopening to traffic (KDOT, 2015a). Many states have similar opening-strength requirements. For overnight repairs, strength targets must be met in 4–6 hours because the contractor must remove the deteriorated pavement, clean the area, mix and pour concrete, and finish the surface before opening the facility to traffic. Many projects require high early-strength concrete (HESC) for pavement repairs to minimize downtime and disruption to traffic. Unfortunately, however, HESC mixtures often demonstrate poor durability in the field. In fact, repaired patches in Kansas have shown premature deterioration, with some patches lasting

only 5–10 years despite their longer life expectancies. Therefore, HESC durability requires further research to increase effective implementation.

1.1 Background

HESC is often used for pavement repairs to avoid extended road closures and to obtain required pavement strength. High cement content is usually combined with a low water-to-cement ratio (w/c) and chemical admixtures, especially hydration-accelerating admixtures (Shanahan et al., 2016). Premature deterioration of concrete pavement (i.e., within 5–10 years) which is less that the planned service life is the case in Kansas. Because financial resources are always a consideration for rehabilitation, a durable rehabilitated concrete pavement with a life expectancy of at least 20 years is essential. Figure 1-1 shows prematurely deteriorated repair slabs in Garden City, Kansas.

Figure 1-1: Prematurely Deteriorated Slabs in Garden City, Kansas

1.2 Problem Statement

Durability in concrete pavement is typically related to shrinkage and freeze-thaw (F/T) cycling. Restrained shrinkage initiates microscopic cracks that are usually the starting path for deterioration because they allow the ingress of water by increasing the effective permeability and diffusivity of the concrete. Relatively low w/c (0.37) has been shown to cause incomplete hydration, resulting in shrinkage, specifically autogenous shrinkage, due to the formation of gel porosity.

In addition to rapid deterioration, HESC has also demonstrated poor resistance to F/T cycles. The exact reason for the observed deterioration is unknown, although cracks have been shown to begin at the corners and joints and propagate within the pavement slab (Li et al., 2011). Factors such as aggregate quality and entrained air content can impact F/T resistance. Contractors often use HESC with high cement content to decrease curing time of the surface and avoid subsequent penalties for delayed road openings, but in doing so, they neglect the potential risk to concrete durability, specifically increased porosity and shrinkage due to high paste/mortar ratios.

Entrained air content most advantageously influences F/T resistance because the entrained air allows space for the frozen water to expand within the concrete matrix, thereby relieving pressure within the concrete and reducing damage associated with F/T cycling. Thus, microcracking related to shrinkage and poor entrained air content within concrete could critically decrease the durability of concrete pavement, especially in Kansas, where pavement routinely experiences severe exposure to F/T cycles.

1.3 Objective

The main objective of this research is to examine the effectiveness of internal curing (IC) to enhance cement hydration and mitigate concrete porosity. Enhancing the microstructure of

concrete reduces shrinkage, which leads to the progression of cracks; these cracks allow the ingress of detrimental chemical substances and decrease F/T resistance. Therefore, this study utilizes Kansas test method KTMR-22, which simulates 20 years of F/T exposure, to investigate the impact of IC on shrinkage and F/T resistance (KDOT 2015b). The acquisition of HESC using IC is essential because the strength, is KDOT'S primary restriction for producing concrete for patching. This study also utilizes a matrix of various cement contents to identify the effects of cement content on concrete mix performance.

Chapter 2 - Literature Review

This chapter reviews concrete damage scenarios and solutions to enhance concrete performance, focusing specifically on HESC and the IC technique.

2.1 Early Concrete Pavement Damage

Concrete performance is defined by the complex relationship between concrete strength and concrete durability. Researchers who have investigated the correlation between strength and durability, such as transport properties that affect durability, have found a direct relationship between concrete strength and concrete durability (Armaghani et al., 1992; Baghabra Al-Amoudi et al., 2009). High-strength concrete pavement deteriorates prematurely due to shrinkage, F/T cycling, and occasionally high repetitions of applied loads. All these mechanisms facilitate the ingress of water and inimical substances, especially at pavement joints. The water expands and exerts tensile stresses on concrete, and the inimical substances corrode the existing steel and cause rust that also induces residual tensile stresses on concrete due to expansion. Those mechanisms do not happen immediately, however; they occur over time and during cycles. In addition to concrete ingredients, mix design procedure, and site execution, environmental exposure also impacts concrete durability.

2.2 Crack Development

Researchers have studied microstructure properties, aggregate fraction and size, F/T cycling, and joints and sealants to evaluate the role transport properties play in initiating deterioration.

2.2.1 Microstructure

As mentioned, microcracks resulting from concrete degradation compromise concrete durability by facilitating the ingress of detrimental agents. However, few studies have directly

correlated microcrack characteristics to mass transport properties (Şahmaran Mustafa & Li, 2009; Wu et al., 2015; Yang et al., 2006). Microcracks typically distribute through cement paste or along the interface of paste aggregate, moving from one particle to another, where they arrest or spread around the aggregate particles. Microcracks rarely penetrate aggregates (Wu et al., 2019). However, theoretical and experimental studies have shown that the effect of microcracking on diffusion is minimal compared to the effect of pressure-induced flow because diffusivity is related to total porosity, whereas permeability depends on pore size and interconnectivity (Gérard & Marchand, 2000; Wong et al., 2007, 2009).

Although HESC has a relatively low water-to-cementitious ratio (w/cem) (i.e., lower than 0.40), Mindess et al. (2003) found that w/cem less than 0.42 results in incomplete hydration, leaving cement unhydrated and self-desiccated. Because intrinsic porosity and development of an interfacial transition zone (ITZ) around any impedance are inevitable, however, a limited amount of permeability and diffusivity may be beneficial for concrete durability. ITZ, a significant source of porosity in cement paste, influences concrete durability while it influences transport properties. Modeling has shown that the ITZ creates an interconnected network even for a modest width of 10–20 μm (Winslow et al., 1994). In addition, experimental study on mortars has shown an increase in paste porosity due to porous ITZs (Delagrave et al., 1997). However, an experimental study on mortars and concretes revealed no definitive conclusion as to whether the ITZ affects bulk transport properties, even if the ITZ is changed systemically by increasing the aggregate content (Wong et al., 2009). A few studies found that the ITZ significantly affects chloride diffusivity (Asbridge et al., 2001; Halamickova et al., 1995), while other studies found opposing results (Buenfeld & Okundi, 1998; Delagrave et al., 1997; Hornain et al., 1995). These conflicting

observations were attributed to parameters such as cement paste fraction and/or aggregate size that affect transport properties and microstructure formation within the concrete.

2.2.2 Aggregate Size and Volume Fraction

Several studies have evaluated the influence of aggregate size, volume fraction, and morphology, as well as the presence of the ITZ, on transport properties. Wong et al. (2009) enhanced the understanding of links between transport properties and microstructure by investigating the relative influences of ITZ and microcracking on oxygen permeability, oxygen diffusivity, and water sorptivity. Batches of paste, mortar, and concrete with w/c 0.30 and w/c 0.50 were compared, and oxygen diffusivity, oxygen permeability, and water sorptivity tests were carried out. Results showed that when the sand content by volume increased in mortars from 0% to 70%, water sorptivity and oxygen diffusivity decreased by a factor of 4–6 and 2–4, respectively, whereas oxygen permeability decreased by a factor of 30–70. The trend was consistent regardless of the w/c (0.3 or 0.5). Concrete had roughly the same sorptivity and diffusivity as its analogous mortar, but permeability was higher (1–2 orders of magnitude) even though it had approximately one-third less ITZ. Results suggest that the high permeability was due to more microcracks that form in concrete compared to mortar when both were exposed to the same drying conditions.

Wong et al. (2009) also observed that increasing aggregate size for the same aggregate content in the mixture increased permeability of concrete. This result is surprising because an increase in aggregate size is usually accompanied by a decrease in the volume of ITZ, which is more porous than cement paste. One hypothesis is that an increase of aggregate diameter results in increased microcrack width, which is closely related to permeability (Witherspoon et al., 1980). Therefore, high permeability in concrete cannot be solely attributed to the ITZ because it would have consequently had a more significant impact on the mortars. Similarly, Herve and Zaoui

(1993) found that changes in total paste volume and total porosity due to mix design and curing had a significant effect on diffusivity. Increasing aggregate content produced ITZ and decreased total porosity because non-porous aggregate particles replaced paste.

Grassl et al. (2010) applied the nonlinear finite element method to analyze shrinkage-induced microcracking of concrete. Their study results concurred with results by Wong et al. (2009): (i) increasing aggregate diameter and volume fraction decreases the length of microcracks; (ii) increasing aggregate diameter and decreasing volume fraction increases average crack width; and (iii) increasing aggregate diameter and decreasing volume fraction increases permeability, which is related to the cube of the crack width.

2.2.3 Mechanical Loading and Freeze-Thaw Mechanisms

Yang et al. (2006) compared mechanical loading and F/T-induced damages to determine how cracking influences transport properties of concrete. After cutting the specimens into slices, electrical conductivity, water absorption, and sorpitivity were used to assess changes in transport properties after a certain degree of tensile loading and a certain number of F/T cycles. Acoustic emission was used to quantify the extent of damage in specimens exposed to tensile loading, while resonant frequency was used to quantify the extent of damage in specimens exposed to F/T. A scanning electron microscope and an optical microscope under high magnification were used to examine microstructure and crack patterns. Results showed that paste cracks or nonconnected interfacial occurred due to mechanical loading up to 80%–90%, meaning that water absorption increased locally and did not substantially influence overall water absorption. In contrast, the crack network was well distributed due to damage induced by F/T, causing the rate of water absorption and electrical conductivity to increase two to three times with increased F/T damage.

Jacobsen et al. (1996) studied the effects of F/T-induced cracks on chloride transport within concrete and found that the chloride penetration rate increased 2.5–8 times compared to undamaged specimens. In addition, Hearn (1999) showed that concrete permeability increased due to certain types of cracks and that drying shrinkage caused water transport in concrete to increase significantly, whereas load-induced damage was unaffected by water permeability. F/T damage that initiates from non-durable aggregate sources is known as durability cracking, or D-cracking. D-cracking often causes deterioration in certain spots in pavement due to poor materials (Fakhri et al., 2017). For example, the use of deicing chemical has been shown to increase the rate and severity of F/T-initiated concrete damage (Suraneni et al., 2016).

Regardless of the initiation source for individual cracks, the resulting damage allows the ingress of detrimental substances into the concrete slab, causing further deterioration. Although excessive shrinkage is a potential source of concrete damage since it promotes crack development, recent research has linked increased transport properties and the degree of damage to concrete (Suraneni et al., 2016).

2.2.4 Joints and Sealants

Joint deterioration investigations in Midwestern states have confirmed that concrete pavement damage typically initiates from pavement joints due to high moisture ingress at these locations (Sutter et al., 2006; Weiss et al., 2007). Joint damage is often attributed to cracking that develops parallel to the joint or spalling at the joint; damage rarely occurs at the pavement surface unless the degree of damage is severe and propagates upward.

Li et al. (2011) investigated the influence of entrained air in concrete on increasing F/T resistivity and joint integrity. They hypothesized that specific joint geometries are more prone to storing water, thereby increasing saturation and initiating local damage. The researchers

specifically studied the degree of saturation and critical flow distance, or maximum distance needed for water to flow from a freezing site to the nearest air-filled void (Figure 2-1).

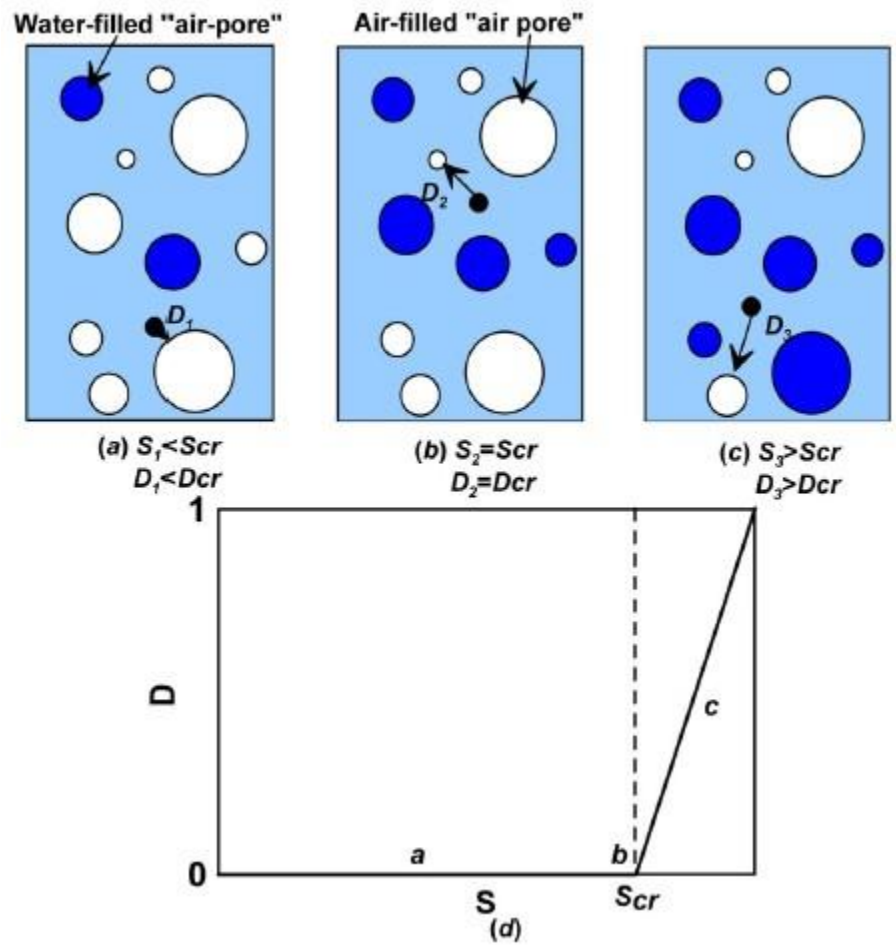

Figure 2-1: Schematic of Relation between Degree of Saturation and F/T Damage

The three mortar mixtures in the figure were prepared with unique air contents (i.e., 13%, 22%, and 31%) and subjected to water absorption and F/T tests. Specimens were conditioned at three levels of relative humidity (RH) (i.e., 50%, 65%, and 80%) for the absorption test, and the F/T test used one daily cycle that consisted of a 2-hour transition, 10 hours at 10 ± 1 °C, another 2-hour transition, and 10 hours at -18 ± 1 °C. Results showed that the absorption rate of the air entrained concrete was higher than a non-air system at later ages, although the absorption rate was

similar at earlier ages for non-air entrained and air entrained systems. In addition, the non-air entrained system took 4–6 days to reach 88% saturation, whereas the air entrained system took 3–6 years to reach that degree of saturation. Surprisingly, exceeding the critical degree of saturation led to failure in all mixtures at each air content volume, meaning that air volume and the air void system would not prevent failure resulting from F/T (Li et al., 2011).

Joints are critical to pavement health as they are the primary pathways for water to flow underneath the concrete pavement. Therefore, effective water infiltration prevention is essential. Sealants, if installed properly, prevent water from penetrating through the joints. Shackel & Yamin (1994) examined the rate of water penetration through joints for various cross slopes. Results showed that, although 65% of rainfall penetrated the joints, that percentage decreased by 50% if joints were sealed.

Sealants are made of compressible materials that can resist compression and tension and provide a waterproof barrier against infiltrated water. Degraded sealants typically cause pavement distresses. Fine-aggregate pumping causes faulting, which eventually leads to cracking, and corrosion of embedded tie and dowel bars which eventually hasten joint deterioration and crack propagation due to improper load transfer. Bad performance can also be attributed to incompressible materials lodged in the joints, causing nonuniform stresses that lead to spalling at the edge, joint, or bottom of the slab in slab expansion (Ray, 1980).

2.3 High Early-Strength Concrete

HESC production typically involves hydration acceleration admixtures. Porras et al. (2020) produced HESC that meets KDOT requirements of 1,800 psi 6 hours prior to opening roads to traffic, at least 4,000 psi after 28 days, and ability to sustain 660 cycles of F/T simulation of a 20-year service life (KDOT, 2015b). The researchers used a 1% and 2% calcium chloride accelerator

with Type III cement (CEM III) with a water reducer to maintain a practical workable concrete and an air entrainer to provide 6.5±1.5% air content. Mixtures with 564 lb, 658 lb, and 752 lb cement contents and w/c of 0.37 were mixed with two dosage rates of calcium chloride to create an experimental matrix of six mixtures. Compressive strength ASTM C39 (2018a), drying shrinkage test ASTM C157 (2017a), surface resistivity KDOT KT-79 (2012), and F/T ASTM C666 (2015a) and KTMR-22 tests were conducted, and the relative dynamic modulus of elasticity (RDME) was measured. Results showed that compressive strength of 1,800 psi was achieved at 4 hours with 2% calcium chloride. The surface resistivity test showed unexpected results, and drying shrinkage was higher for mixtures with 1% calcium chloride than mixtures with 2% calcium chloride. The mixture with the lowest cement content and 2% accelerator demonstrated the best durability because it had the least expansion and lowest RDME reduction over 659 cycles based on the specified threshold.

Cements such as calcium sulfoaluminate (CSA) and magnesium phosphate cements are emerging as alternatives for ordinary Portland cement when producing HESC. Each cement is categorized based on compressive strength, setting time, and other physical and chemical characteristics according to ASTM C1600 (2019a). CSA cement has high amounts of aluminum oxide (alumina, Al_2O3) and sulfur trioxide (SO_3), which contribute to very high strength gain over a very short time.

Guan et al. (2017) investigated the feasibility of using CSA cement for concrete pavement repair patches. Mixtures utilized various cement contents and w/c but an identical aggregate source and content, and the investigation was based on strength development, shrinkage, and the coefficient of thermal expansion. Figure 2-2 shows that the strength of CSA cement was higher at early ages, especially during the first day when it attained more than 3,000 psi within 4 hours after

mixing. Although Figure 2-3 shows that CSA cement shrinkage was less than CEM III shrinkage, the coefficient of thermal expansion was the same for both concrete mixtures because thermal expansion is typically dominated by coarse aggregates, and the aggregate contents were identical for both mixtures in this study.

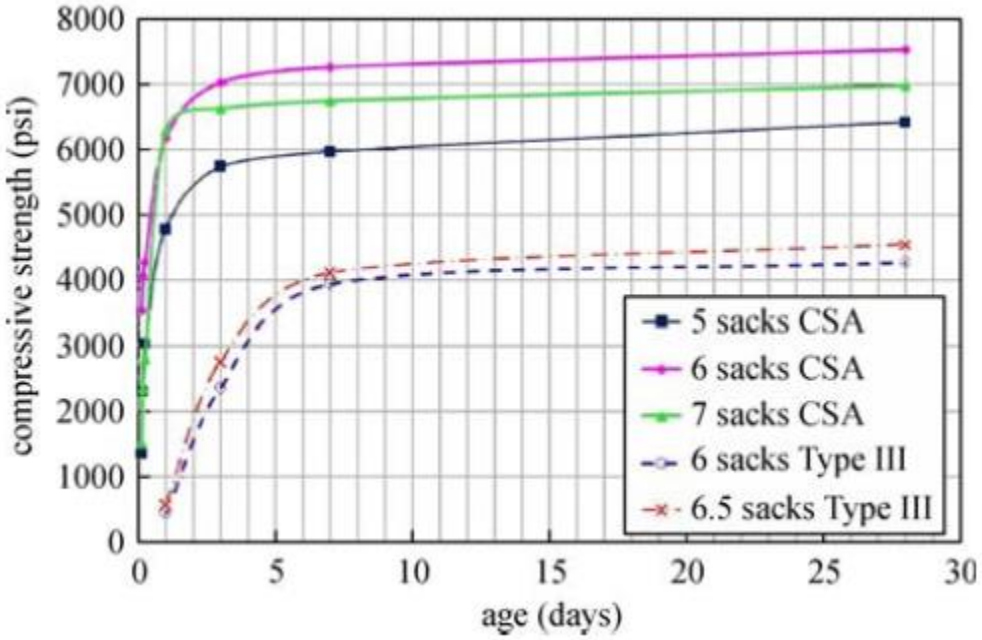

Figure 2-2: Compressive Strength for CSA and CEM III Concretes at w/c 0.45 (Guan et al., 2017)

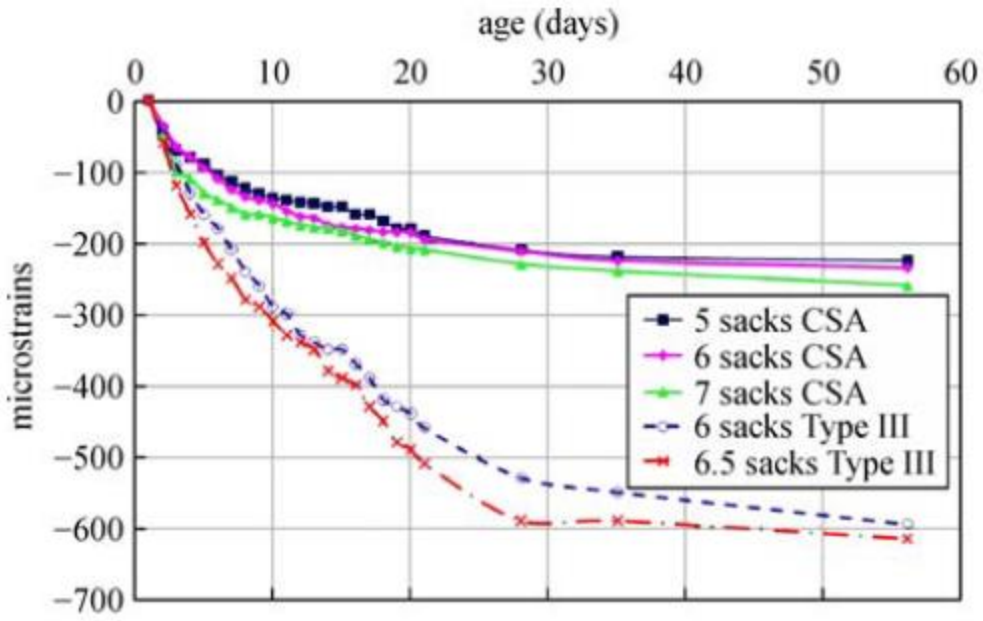

Figure 2-3: Shrinkage for CSA and CEM III Concretes at w/c 0.45 (Guan et al., 2017)

2.4 Durability Practices

Much research has investigated various approaches to improve concrete durability, including densifying the microstructure, improving the mechanical properties, and improving curing. The following section describes the use of IC to improve densification.

2.4.1 Supplementary Cementitious Material

The use of supplementary cementitious materials (SCMs) can increase the packing density of C-S-H, which decreases the ITZ and produces less porous medium. Saraswathy & Song (2007) used rice husk ash (RHA) as a SCM. RHA replacements of 0%, 5%, 10%, 15%, 20%, 25%, and 30% were blended with Type I cement and tested after being cured in water for 28 days. Several tests were done to assess the compressive strength, effective porosity according to ASTM C642-97 (1997), and water permeability and chloride penetration resistance using the rapid chloride penetration test ASTM C1202-94 (2019b). Table 2-1 shows that the compressive strengths of the replacements were similar to the control. Table 2-2 and

Table 2-3 show the reduction in effective porosity and chloride diffusivity calculated in terms of coulombs as evidence for improved porosity. Results showed that the increasing level of RHA percentage enhanced the transport properties.

Table 2-1: Compressive Strength of RHA (Saraswathy & Song, 2007)

% of replacement	Average compressive strength (N/m^2)		
	7 days	14 days	28 days
0(OPC)	27.22	33.29	36.45
5	31.32	35.62	36.49
10	30.45	35.97	37.43
15	31.52	35.04	37.38
20	31.64	36.17	37.71
25	33.09	35.27	39.55
30	33.53	35.44	37.80

Table 2-2: Porosity of RHA (Saraswathy & Song, 2007)

Sl. no.	**% of replacement**	**Effective porosity**
1	**Type I cement**	18.06
2	5	18.18
3	10	13.82
4	15	13.8
5	20	13.54
6	25	13.04
7	30	11.89

Table 2-3: Chloride Diffusivity of RHA (Saraswathy & Song, 2007)

SI. no.	% of replacement	Charged passed in coulombs
1	**OPC**	1161
2	5	1108
3	10	653
4	15	309
5	20	265
6	25	213
7	30	273

2.4.2 Nano Particles

Shekari & Razzaghi (2011) studied the effects of replacing Type I cement with fixed amounts of nano ZrO_2 (NZ), nano Fe_3O_4 (NF), nano TiO_2 (NT), and nanoAl_2O_3 (NA) in concrete mixtures. Type I cement, metakaolin, and nano particles were used. The metakaolin content of each mixture was 15% of the cementitious material, and the range of nano particle sizes varied from 10 to 25 nanometers. The nano particle content in each mixture was 1.5% by weight of the cementitious materials. Compressive strength, water absorption per ASTM C642, and chloride penetration per ASTM C1202-97 were measured with satisfactory results, as shown in Table 2-4, Figure 2-4, and Figure 2-5, respectively.

Table 2-4: Compressive Strength of Specimens after 28 Days (Shekari & Razzaghi, 2011)

Specimen	Compressive Strength (MPa)
C	92.3
NZ	110.9
NT	113.3
NA	143.1
NF	119.0

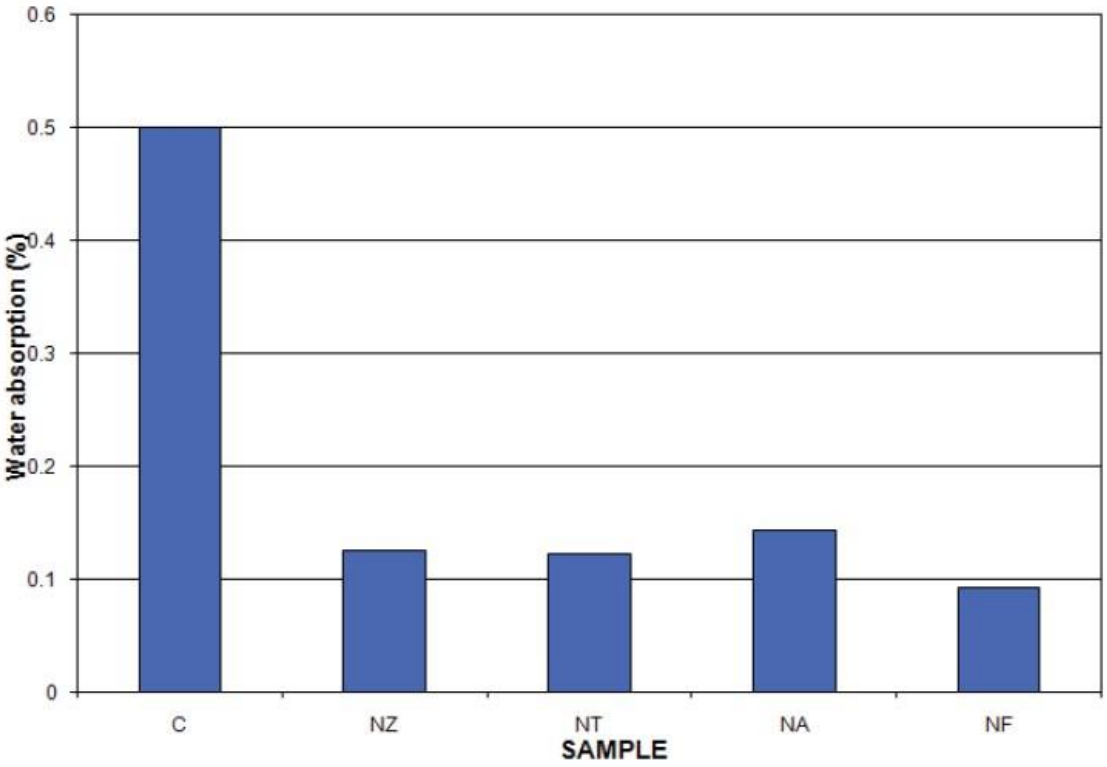

Figure 2-4: Water Absorption of Specimens (%) (Shekari & Razzaghi, 2011)

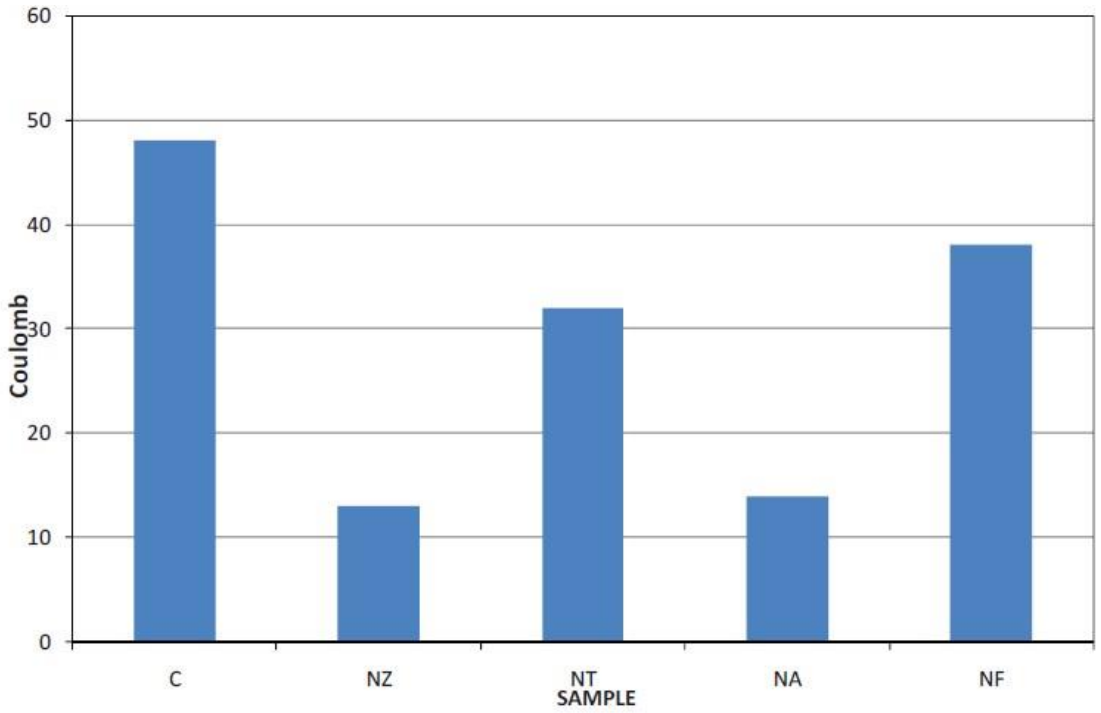

Figure 2-5: Chloride Penetration in Examined Specimens (Shekari & Razzaghi, 2011)

Table 2-4 shows that specimen NA demonstrated the highest compressive strength, and specimens NF and NZ demonstrated effective transport properties. However, any kind of nano particles would improve concrete durability and strength.

2.4.3 Engineering Cementitious Composites

Restrained shrinkage-induced damage and loading-induced damage produce cracks because they cause the tensile strength capacity of concrete to be exceeded. Shrinkage can be restrained internally using aggregates or externally via restrained concrete pavement. Improved ductility that leads to increased tensile strength capacity of concrete is essential, especially for the internal restriction by the aggregates (Li & Li, 2009). Concrete mixtures that contain engineered cementitious composites (ECC) have demonstrated substantial reductions in crack width and increased concrete durability due to the high tensile capacity of fiber-reinforced concrete that exhibits metal-like tensile response with ultra-high tensile strain capacity of 3%–5%,

approximately 300–500 times the tensile strain capacity of normal concrete and fiber-reinforced concrete.

2.5 Internal Curing

While concrete is fresh, it typically loses water through evaporation. Self-desiccation initially occurs inside the core of the concrete, leading to incomplete hydration for the cement grains due to water shortages. Therefore, effective curing of the concrete is critical. The American Concrete Institute (ACI) defines curing as "action taken to maintain moisture and temperature conditions in a freshly placed cementitious mixture to allow hydraulic cement hydration and (if applicable) pozzolanic reactions to occur so that the potential properties of the mixture may develop" (ACI, 2013). Unfortunately, however, because water provided by external curing does not penetrate more than a few millimeters into the concrete surface, the full thickness of the concrete is not cured, especially in highly dense concrete, potentially resulting in concrete warping (Jeong & Zollinger, 2004). Philleo (1991) stated that, "Either the basic nature of Portland cement must be changed so that self-desiccation is reduced, or a way must be found to get curing water into the interior of high strength structural members." The basic nature of Portland cement is the nature of reaction and unable to be changed, but the latter is possible when saturated lightweight aggregates (LWA) are used via IC.

High-strength concrete at low w/c tends to develop gel pores due to lack of available water to hydrate all cement grains. Therefore, the net volume of hydrated products becomes less than the bulk volume of reactants, causing chemical shrinkage and subsequent physical shrinkage (Barcelo et al., 1999; Mindess et al., 2003; Sant et al., 2009). This current research attempted to use IC for providing the needed water to avert chemical shrinkage. ACI defined IC as "supplying water throughout a freshly placed cementitious mixture using reservoirs, via pre-wetted LWA, that

readily release water as needed for hydration or to replace moisture lost through evaporation or self-desiccation" (ACI, 2010). Crushed concrete aggregates (CCA), superabsorbent polymers, and wood fibers have high absorption-desorption capabilities within a certain RH and could also be used to provide additional water instead of LWA.

The addition of water to the concrete via pre-wetted aggregates enhances cement hydration without affecting mixture properties. Cleary & Delatte (2008) found that the cracking risk decreased when pre-wetted LWA added water to prolong cement hydration without changing the w/c. In addition to hydration enhancement, IC is expected to increase resistance to early-age cracking and enhance durability. Bentz & Weiss (2011) found that early-age shrinkage, including autogenous and plastic shrinkage, was completely eliminated and drying shrinkage was mitigated and delayed when IC was used. Autogenous shrinkage is more critical than drying shrinkage for high-strength concrete since autogenous shrinkage increases with decreased w/c (Zhang et al., 2003) and drying shrinkage increases with increased w/c due to the evaporation of water (Mindess et al., 2003). Bentz & Stutzman (2008) used scanning electron microscopy to examine blended cement with and without IC. Results showed that mixtures with internal IC had fewer and smaller empty pores and unhydrated cement grains, as well as a homogenous and dense ITZ between the cement paste and the LWA.

2.5.1 Proportioning

Additional water that is needed to maintain saturated conditions within the hydrated cement paste for a long time of hydration contributes to a higher degree of cement hydration and reaction of any pozzolan and reduces autogenous shrinkage and early-age cracking with strains (Bentz & Weiss, 2011). The needed amount of extra water provided by internal reservoirs is primarily dependent on sorption capacity of the internal reservoir at relatively high RH, absorption degree

of the internal reservoir, and chemical shrinkage of the cement or pozzolan if proper spatial distribution within the cement matrix is available (Bentz & Weiss, 2011).

Bentz & Snyder (1999) developed the following equation to equate water demand of the hydrating mixture to the supply provided by the internal reservoirs:

$$MLWA = \frac{Cf * CS * a\ max}{S * \ \emptyset LWA} \quad (1)$$

where,

MLWA = mass of (dry) fine LWA needed per unit volume of concrete (kg/m3 or lb/yd3);

Cf = cement factor (content) for concrete mixture (kg/m3 or lb/yd3);

CS = chemical shrinkage of cement (g of water/g of cement or lb/lb);

$a\ max$ = maximum expected degree of cement hydration (based on w/c 0.36);

S = degree of saturation of aggregate (0 to 1); and

$\emptyset LWA$ = absorption of LWA (kg water/kg dry LWA or lb/lb).

The desorption of water from LWA to the surrounding cement paste is contingent upon water moving from large pores to small pores. One restriction of the IC technique is the desorption capability of pre-wetted LWA. Castro et al. (2011) determined that, although most LWA can desorb relatively 90% of water at RH > 93%, an increase of 25% in LWA mass is required for nondesirable LWA. Figure 2-6 shows the desorption capacity of desirable and nondesirable LWA.

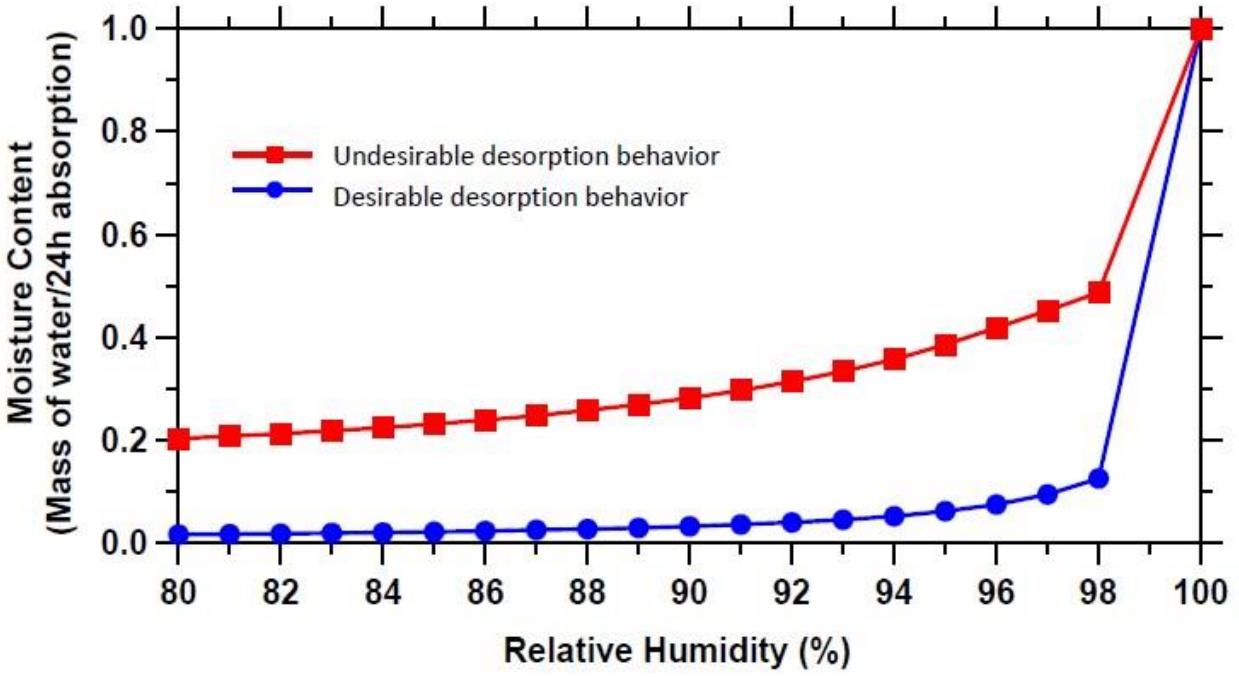

Figure 2-6: Desirable and Undesirable Aggregate Desorption Behavior (Castro, 2011)

Fine or coarse pre-wetted aggregates can be used as IC aggregates, but fine pre-wetted aggregates improve aggregate distribution, resulting in reduced distance between aggregates, a higher fraction of internally cured cement, and overall increased densification of C-S-H compared to mixtures with coarse pre-wetted aggregates (Henkensiefken et al., 2011; Philleo, 1991). Bentz et al. (2007) created Table 2-5 to estimate the travel distances of water particles from the reservoir to the surrounding cement according to hydration age.

Table 2-5: Distances Water Traveled from Surfaces of Internal Reservoirs (Bentz et al., 2007)

Hydration age	Estimated travel distance of water
Early (i.e., < 1 day)	20 mm
Middle (i.e., 1 day to 3 days)	5 mm
Late (i.e., 3 days to 7 days)	1 mm
Worst case (i.e., > 28 days)	0.25 mm

Henkensiefken et al. (2009b) used a hard core/soft shell model to model 16 mixtures with different aggregate sizes and fineness modulus values. Figure 2-7 shows the values of protected paste in concrete for 30% replacement of fine or coarse aggregates with travel distance limited to 2 mm. Results showed that the protected fraction of the paste was 50% with coarse aggregate, while nearly all the paste was protected with fine aggregate. Therefore, "fine LWA is preferred to coarse LWA since it will have a smaller distance between the aggregates and will, therefore, provide the beneficial effects of IC to a greater volume of paste" (Henkensiefken et al., 2009b).

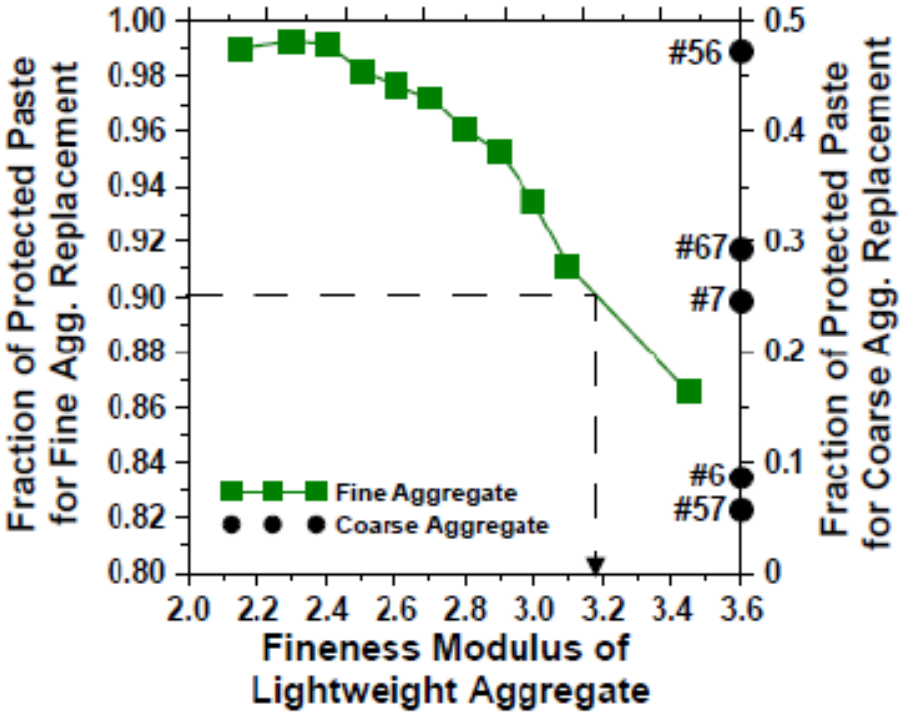

Figure 2-7: Fitness Modulus Values and Volume of Protected Paste in Concrete with 30% Aggregate Replaced with Coarse Aggregate or Sand (Henkensiefken et al., 2009b)

2.5.2 Strength and Elastic Modulus

2.5.2.1 Compressive Strength

Although the effect of IC on concrete strength has been shown to decrease and increase, the general trend is that early-age concrete strength with IC is less than counterparts without IC,

but late-age concrete strength is higher with IC. The New York State Department of Transportation (NYSDOT) used 30% LWA and w/c 0.40 to construct several bridges using IC. Table 2-6 shows the resulting compressive strengths as reported by Streeter et al. (2012).

Table 2-6: Concrete Properties for NYSDOT Bridges (Streeter et al., 2012)

		7-Day Strength (psi)		28-Day Strength (psi)		56-Day Strength (psi)	
Highway	Feature spanned	Control	IC	Control	IC	Control	IC
I-81	End Hill Road	3,720	3,335	5,040	5,273	5,900	5,853
I-290 Ramp D	I-290	3,040	3,500	4,677	4,683	5,343	5,417
Court Street	I-81	4,727	4,859	6,309	6,976	nd	nd

Liu et al. (2017) used superabsorbent polymers (SAP) and LWA to provide IC for high-performance concrete. Results showed that, although internal reservoirs provide extra water to improve the microstructure of cement paste, the pores are relatively big, and when they empty, they contribute to a decrease in compressive strength compared to high-performance concrete without IC.

2.5.2.2 Flexural Strength

Justs et al. (2015) produced internally cured ultra-high-performance concrete using SAP. They utilized several mixtures with different w/c to investigate strength development at various ages compared to the control mixture. IC was used for mixtures UHPC-0.183SAP and UHPC-0.2SAP; the remaining mixtures were controls. Figure 2-8 shows a decrease in flexural strength for mixtures with IC compared to mixtures without IC due to intrinsic weak SAP and the formation of voids once SAP empty.

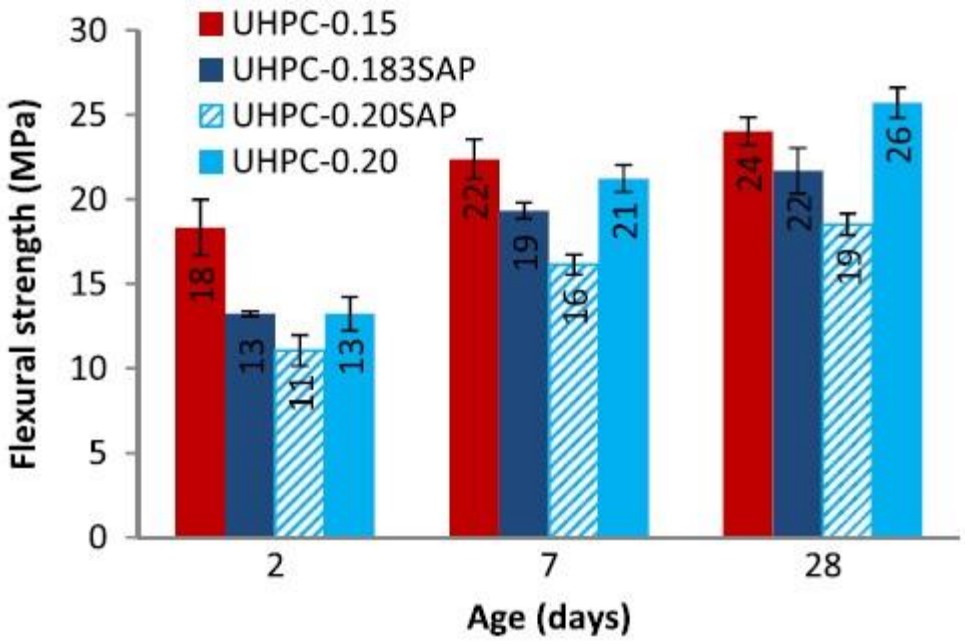

Figure 2-8: Flexural Strength of UHPC with w/c and SAP (Justs et al., 2015)

2.5.2.3 Modulus of Elasticity

Golias (2010) investigated the effect of IC on the modulus of elasticity of concrete. Plain (P) and IC mixtures with w/c of 0.3 and 0.5, respectively, were prepared. Results showed a reduction in the modulus of elasticity (Figure 2-9) that was attributed to the lower stiffness of LWA compared to natural aggregates.

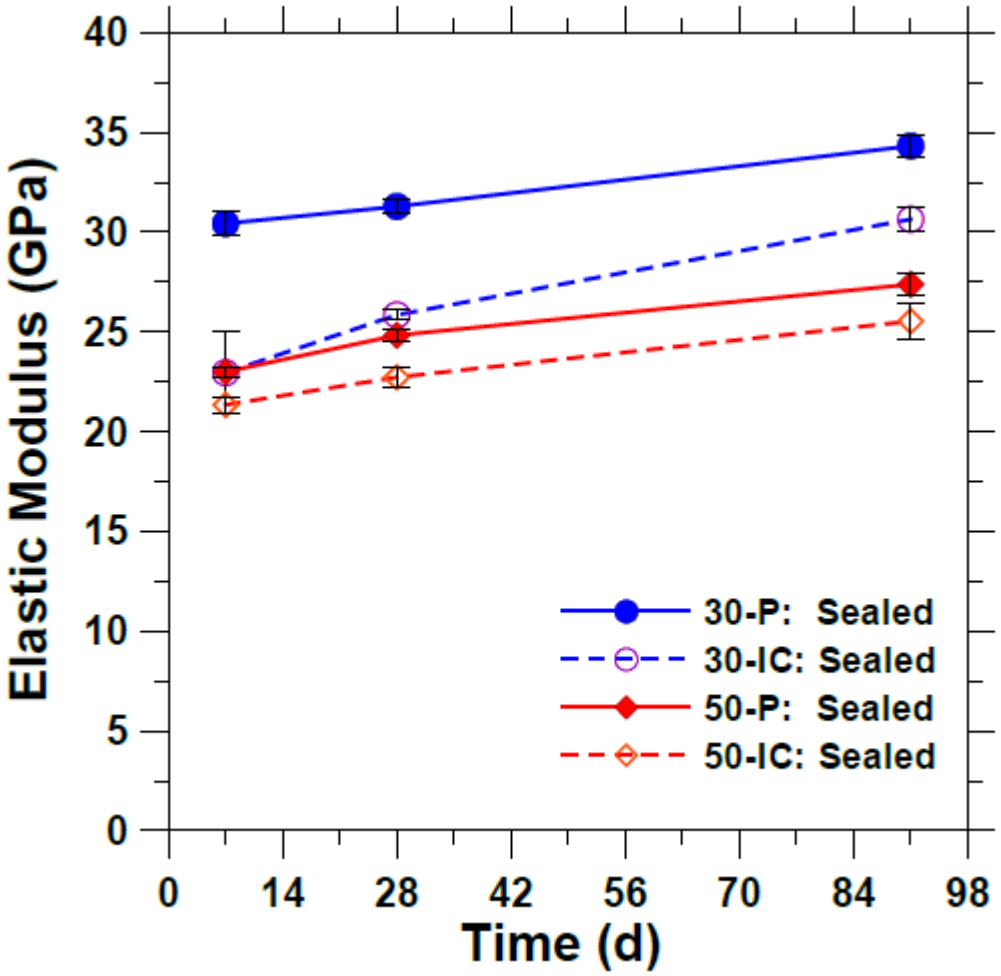

Figure 2-9: Elastic Modulus of Sealed Specimens after IC (Golias, 2010)

2.5.3 Shrinkage Mitigation

In general, three kinds of shrinkages occur in concrete. Plastic shrinkage takes place while concrete is still fresh, and autogenous and drying shrinkages take place when the concrete hardens.

2.5.3.1 Plastic Shrinkage

Plastic shrinkage occurs due to the evaporation of water bleeding from the concrete surface while concrete is hardening. During hardening, aggregate and cement particles settle down and force water to rise to the surface. Water typically evaporates from the surface at a constant rate of drying (Lura et al., 2007). If the evaporation rate is higher than the rate of water provided to the

surface by bleeding, capillary stresses in the system occur as a result of drawing water between the particles, resulting in plastic shrinkage cracking. Figure 2-10 conceptually illustrates the mechanism of plastic shrinkage via the drying of water-filled LWA on the concrete surface immediately after placement.

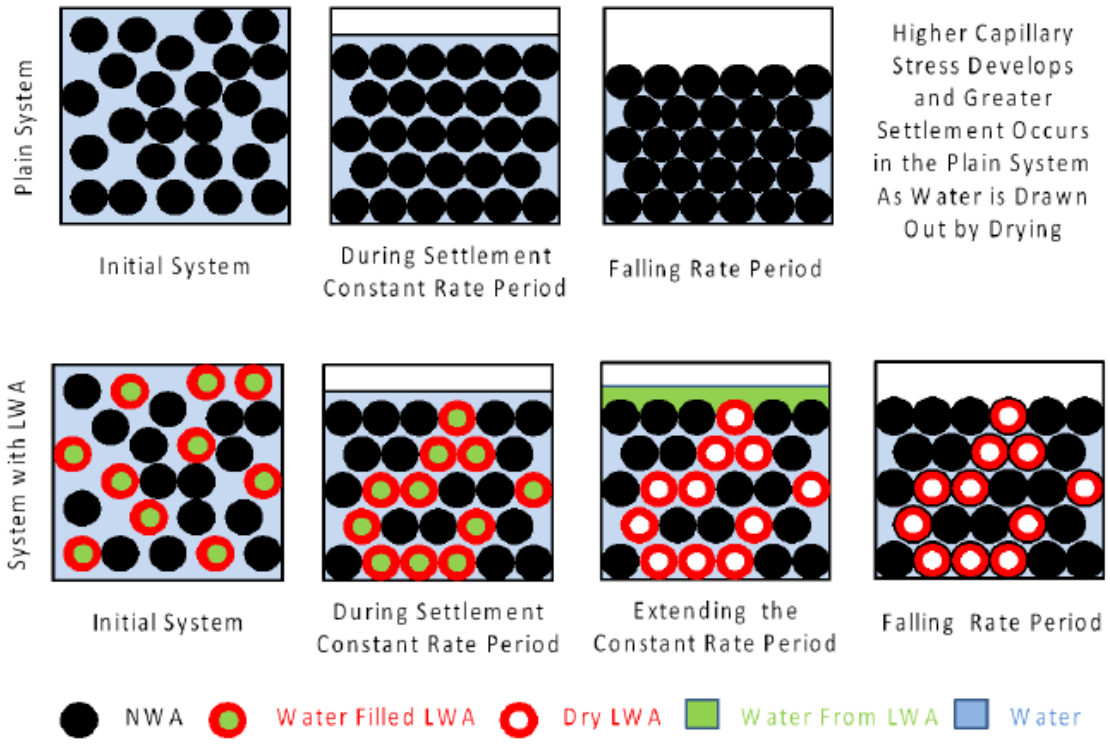

Figure 2-10: Water-Filled LWA Exposed to Drying (Henkensiefken et al., 2010)

Henkensiefken et al. (2010) examined the role of various replacement ratios of LWA for mitigating plastic shrinkage. Results showed that obtaining the required amount of water based on equation (1) (i.e, 18% in Figure 2-11) could completely eliminate plastic shrinkage. However, because water lost when mitigating plastic shrinkage is not available to reduce autogenous and drying shrinkages, extra water must be available to eliminate various types of shrinkage (Bentz & Weiss, 2011).

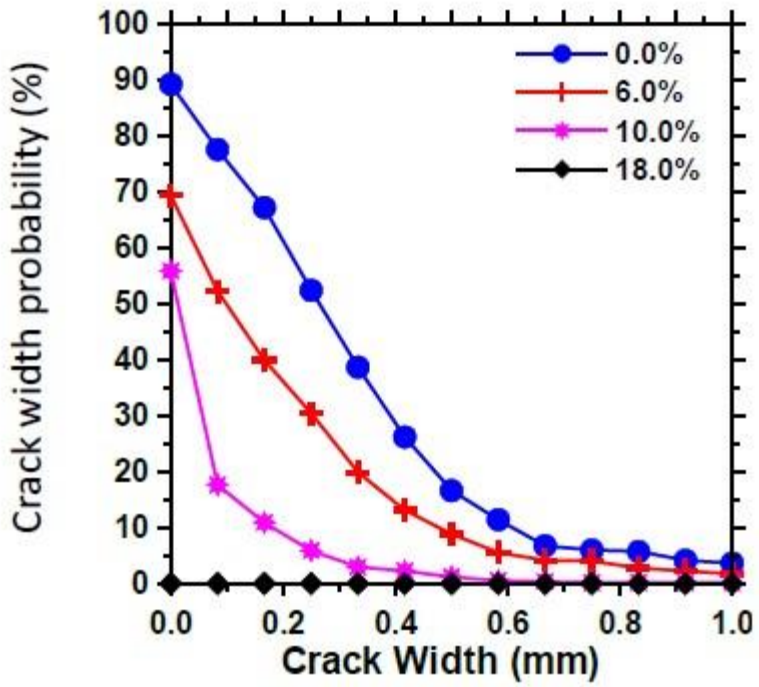

Figure 2-11: Probability Distribution of Crack Width Occurrences in Concrete with Replacement Volumes of Pre-wetted LWA (Henkensiefken et al., 2010)

2.5.3.2 Autogenous Shrinkage

When concrete is hardening, autogenous shrinkage occurs initially, thereby causing cracking at high strain rates. Extra water added to unhydrated cement is thought to reduce or nearly eliminate autogenous shrinkage. Henkensiefken et al. (2009a) investigated the efficacy of IC for reducing autogenous shrinkage. Mortar samples were mixed at w/c = 0.37 and various levels of pre-wetted LWA replacement to provide IC (Figure 2-12). Results showed that LWA replacement of 23.7% was equal to what Bentz & Snyder (1999) suggested as shown in equation (1). As shows, Figure 2-12 autogenous shrinkage decreased significantly as percentage replacements of LWA increased.

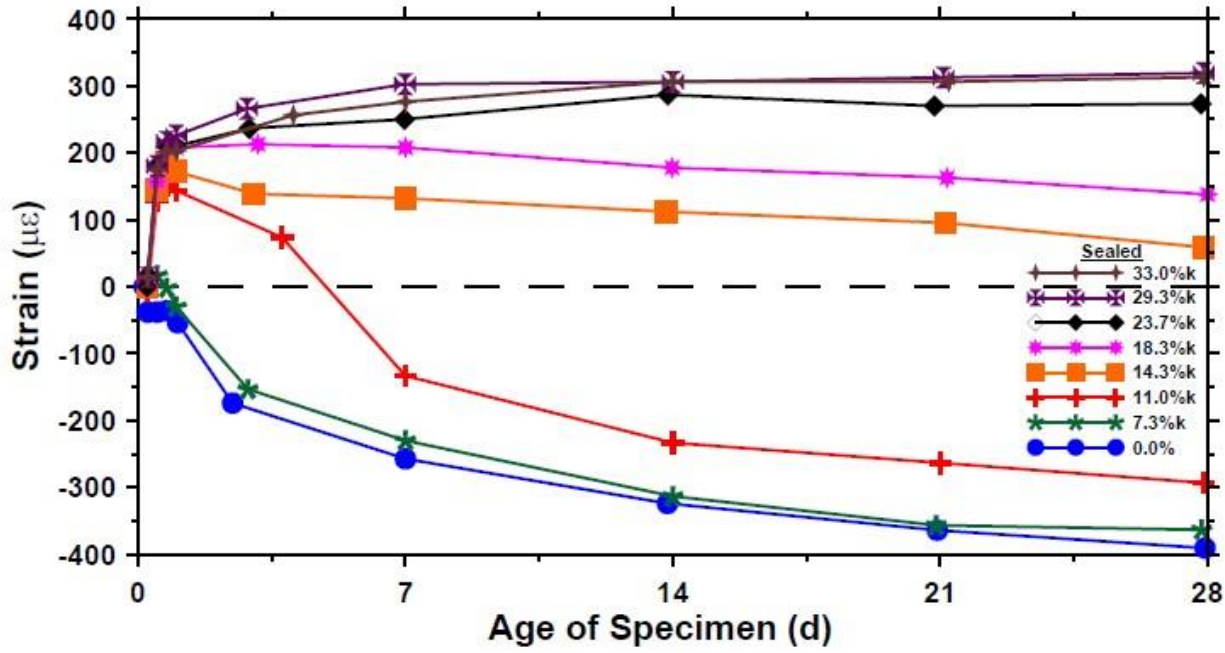

Figure 2-12: Autogenous Deformation Measurements on Cement Mortars (Henkensiefken et al., 2009a)

In the same study, Henkensiefken et al. (2009a) used the ASTM C1581 (2018b) restrained ring shrinkage test to monitor cracking in the mortar samples. Results showed that no cracking occurred for samples with 23.7% or higher replacement percentages (Figure 2-13). A sharp rise in the strain curve in the figure indicates the occurrence of cracking in the specimen.

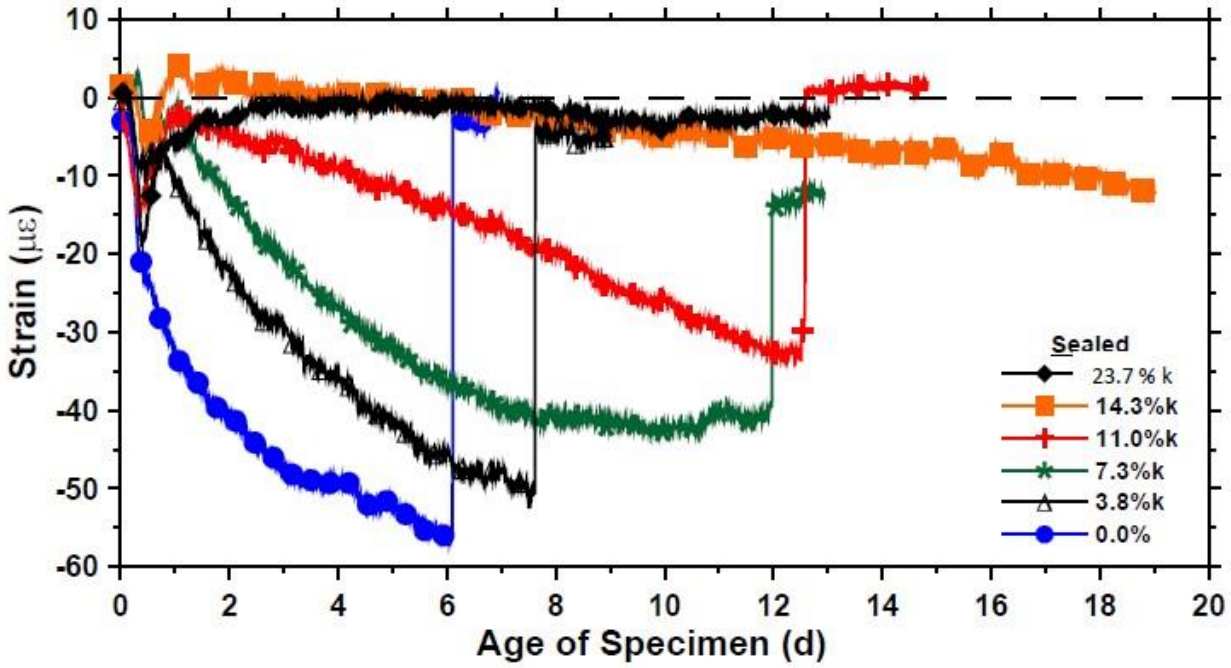

Figure 2-13: Restrained Shrinkage Results for Mortars with Sealed Curing Conditions (Henkensiefken et al., 2009a)

Supporting studies found that autogenous shrinkage could be eliminated and the risk of early-age cracking be reduced (Liu et al., 2017; Shen et al., 2016).

2.5.3.3 Drying Shrinkage

Long-term shrinkage, or drying shrinkage, is the most critical shrinkage for mortars. Henkensiefken et al. (2009a) investigated the effect of IC on mitigating drying shrinkage. Using ASTM C1581, they found that IC delayed crack development and decreased but did not eliminate shrinkage. However, the reduction in drying shrinkage and the delay in crack development increased with increased percentages of LWA replacement, as shown in Figure 2-14 and Figure 2-15, respectively. A sharp vertical rise in the strain curve in Figure 2-15 indicates cracking in the specimen. Similarly, in their investigation of the use of SAP for high-performance internally cured concrete, Liu et al. (2017) found that controlled dosages of SAP and additional water helped mitigate drying shrinkage; otherwise drying shrinkage increased.

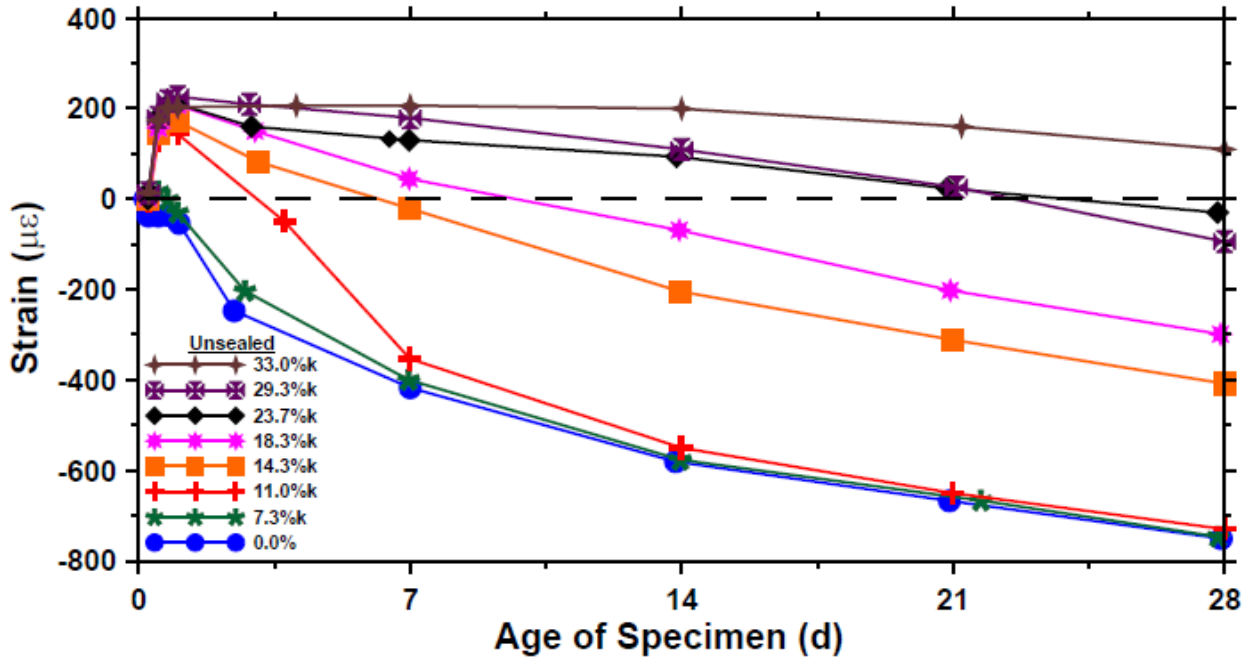

Figure 2-14: Measured Deformation of Free Shrinkage Specimens with Unsealed Curing Conditions (Henkensiefken et al., 2009a)

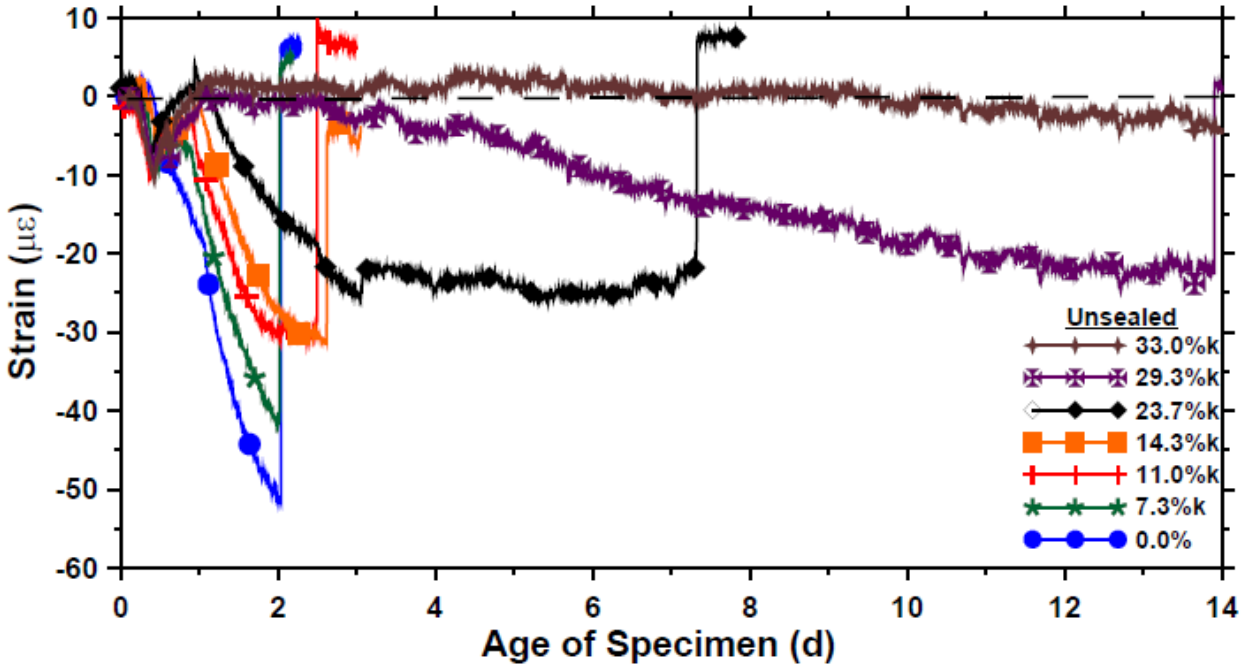

Figure 2-15: Restrained Shrinkage Results for Mortars with Unsealed Curing Conditions. (Henkensiefken et al., 2009a)

2.5.4 Warping

Warping occasionally occurs in concrete pavement due to moisture gradient across the slab; drying shrinkage is a primary cause of moisture gradients (Jeong & Zollinger, 2004; Wei 2008). Wei & Hansen (2008) found that warping decreased 70% for concrete mixes with IC, w/c 0.45, and drying time of 16 days, proving that a uniform RH through the thickness of a concrete slab decreases warping by desorbing water from LWA.

2.5.5 Freezing and Thawing

Many researchers have studied internally cured concrete subjected to F/T damage. Schlitter et al. (2010) investigated internally cured concrete specimens that were cured for 14 days under sealed conditions. Results showed no damage after 300 cycles (two cycles per day with temperature between 10 °C and -18 °C). However, researchers concluded that when water desorbed from the pre-wetted aggregates, air voids were created that may increase F/T resistance.

Moreover, Cusson & Margeson (2010) investigated the IC technique for enhancing concrete performance by exposing concrete specimens to 350 F/T cycles: 300 rapid cycles in water and 50 slow cycles in 4% $CaCl_2$. Improved performance was observed for the concrete with IC, as shown in Table 2-7.

Table 2-7: Impact of IC Properties on High-Performance Concrete (Cusson & Margeson, 2010)

Property	Reference concrete (w/c = 0.35)	Internally cured concrete (w/c = 0.35)	Relative improvement (%)
w/c (kg/kg)	0	0.075	
C-S-H content at 28 days (%)	10.2	12.3	21
Compressive strength at 7 days (Mpa)	45	50	11
Compressive strength at 28 days (Mpa)	60	65	8
Water permeability (m/s)	2.1 * 10-11	1.7 * 10-11	19
Chloride permeability (coulomb)	553	415	25
F/T resistance, mass loss (%)	0.3	0.26	25
Salt scaling resistance, mass loss (%)	0.46	0.3	

2.5.6 Projects with Internally Cured Concrete

2.5.6.1 High Early-Strength ICC Off Ramp of I-635 in Mesquite, Texas

In 2012, a road section in Mesquite, Texas, was constructed using a high-strength concrete and the IC technique. The mixture of CEM III (gap-graded with LWA), water reducer, non-chloride accelerator, and slump-retention admixture decreased shrinkage cracking with no effect on concrete strength (Rao & Darter, 2013).

2.5.6.2 Dallas Intermodal Terminal

In 2005, a large railway transit yard in Dallas, Texas, required 190,000 m^3 internally cured concrete (Villarreal & Crocker, 2007). LWA was blended with natural aggregates, and the IC resulted in a noticeable increase in 28-day strength (>15%) and the elimination of cracking due to plastic and drying shrinkage. In 2007, several crack surveys identified only three cracks in the highway.

2.5.6.3 State Highway 121 North of Dallas, Texas

In 2006, a five-mile section of state highway 121 north of Dallas was constructed. A 13 in of continuous reinforced concrete pavement employed IC technique and was placed using slip-form paving. Flexural and compressive strengths met the requirements set by the Texas Department of Transportation (TxDOT), and 10 months after highway construction completion, a crack survey identified significant reductions in the number of cracks (21 versus 52 in the control mixture without IC) and in the crack widths compared to the control sections (Friggle & Reeves, 2008).

2.5.7 Internal Curing in Practice

The moisture content and absorption capacity of the LWA determines the needed amount of LWA to produce the optimal performance of internally cured concrete. Therefore, quality control of moisture content and absorption capacity is vital prior to mixing, although the method to control moisture prior to mixing is less understood. Golias (2010) assessed the influence of oven-dried, 24-hours pre-wetted, and vacuum-saturated LWA. Results showed that the addition of oven-dried or 24-hours pre-wetted LWA had an identical effect on concrete performance; both increased the strength and degree of hydration and decreased autogenous shrinkage and water sorption. Vacuum-saturated LWA, however, demonstrated no significant advantage over the other states since water may be held in the smallest pores and be unable to desorb into the surroundings. Therefore, knowing the moisture content to the highest accuracy prior to mixing is critical, and it substitutes the needed water to achieve the saturated surface.

2.6 Summary

In general, joints are most likely to initially show deterioration in a concrete pavement slab, thereby compromising slab durability. Concrete ingredients significantly affect the microstructure

of the cement matrix within the concrete, and critical sealants and joints must be maintained since they are the point of entry for detrimental substances. Patching requires high early-strength concrete, but the concrete must be durable. Supplementary materials such as chemical admixtures or CSA cement can be used with or instead of ordinary cement to acquire HESC.

This research focused on IC, an emerging method with limited previous research. An equation was developed to determine the amount of additional water needed to prevent chemical shrinkage. Previous literature showed that IC could eliminate plastic and autogenous shrinkage, mitigate drying shrinkage, and delay cracking development. Therefore, this study investigated whether IC could improve F/T resistance in concrete. Although IC did not produce a significant reduction in early-age concrete strength, the IC results were relatively close to the control for late-age concrete. LWA can be used in any state if the moisture content and absorption capacity are known by storing LWA in separate bins to keep them almost dry or sprinkling LWA prior 24 hours to achieve a known moisture content and then adding or deducting water to achieve a saturated-surface dry condition.

Chapter 3 - Materials

This chapter summarizes the characteristics of aggregates, admixtures, accelerators, and CEM III used in this study.

3.1 Aggregates

Fine, coarse, LWA, and CCA aggregates were used in this research.

3.1.1 Fine Aggregates

This research utilized naturally occurring sand (Figure 3-1), and sieve analysis as well as moisture content and specific gravity were calculated according to ASTM C136 (2019c) and ASTM C128-15 (2015b), respectively. Moisture content and oven-dried specific gravity values were 1.41% and 2.587, respectively. Results from the sieve analysis are shown in Table 3-1.

Figure 3-1: Natural Sand-Fine Aggregate

Table 3-1: Sieve Analysis for Fine Aggregates

Sieve #	%passing
3/4"	99
1/2"	88
3/8"	65
#4	9
#8	1
Pan	

3.1.2 Coarse Aggregates

This research also utilized naturally occurring gravel (Figure 3-2), and sieve analysis as well as moisture content and specific gravity were calculated according to ASTM C136 and ASTM C127-15, respectively. Moisture content and dry specific gravity values were 2% and 2.544, respectively. Results from the sieve analysis are shown in Table 3-2.

Figure 3-2: Natural Gravel-Coarse Aggregate

Table 3-2: Sieve Analysis for Coarse Aggregates

Sieve #	%passing
#4	97
#8	85
#16	66
#30	43
#50	18
#100	3
Pan	

3.1.3 Lightweight Aggregates

Quarried clay, slate, or shale are typically crushed into desirable sizes and then fed into a kiln at 1,200℃ (2,200 ˚F). At this high temperature, the materials start to liquefy, and the

carbonaceous compounds form gas bubbles that cause the materials to expand. These materials are then transferred to a cooler that circulates air to solidify the materials to become highly porous (Lightweight Aggregate Manufacturing). Figure 3-3 shows the LWA obtained from Trinity Lightweight LLC in Boulder, Colorado for this study. Sieve analysis as well as moisture content and specific gravity were calculated according to ASTM C136 and ASTM C128-15, respectively, and moisture content and dry specific gravity values were 21.5% and 1.579, respectively. Results of the sieve analysis are shown in Table 3-3.

Figure 3-3: Fine Lightweight Aggregates

Table 3-3: Sieve Analysis for LWA

Sieve #	%passing
#4	100
#8	96
#16	70
#30	48
#50	31
#100	22
#200	17

3.1.4 Crushed Concrete Aggregates

CCA was obtained from pavement at the Kansas City International Airport in Kansas City, Missouri. After being discarded, deteriorated and replaced concrete is often crushed for various aggregate applications. Because this aggregate came from old airfield concrete pavement, it was likely routinely exposed to deicing salts. Figure 3-4 depicts the fine portion after sieving; only fine materials under sieve US No. 4 were used. Sieve analysis as well as moisture content and specific gravity were calculated according to ASTM C136 and ASTM C128-15, respectively. Moisture content and dry specific gravity values were 11% and 2.076, respectively. Results from the sieve analysis are shown in Table 3-4.

Figure 3-4: CCA

Table 3-4: Sieve Analysis for CCA

Sieve #	%passing
#4	99
#8	71
#16	49
#30	32
#50	19
#100	12
#200	9

3.2 Admixtures

This study utilized a water reducer, air entrainer, and accelerator to obtain the required fresh concrete properties and strength within a short time after mixing.

3.2.1 Water Reducer

Because high-strength concrete with low w/c provides a very low slump value, water reducer is often used to improve concrete workability and indirectly increase concrete strength. Cement particles are typically charged with both positive and negative charges, which enhances the attractiveness between particles and leads to particle clusters. With a water reducer, cement particles become charged with an identical single charge, which causes cement particles to repulse each other, thus promoting the dispersion of cement grains and increasing the fluidity of the cement paste. This research used the high-range water reducer ADVA® 140M from GCP Applied Technologies. This water reducer utilizes polycarboxylate technology specifically formulated to meet the needs of the concrete industry, as well as the requirements of ASTM C494 (as a Type A and F) and ASTM C1017 Type I (GRACE, 2007a). Typical addition rates for high-range water reducers are 9–16 oz/cwt of cement.

3.2.2 Air Entrainer

Although vibration is often used to eliminate entrapped air bubbles in concrete, entrained air bubbles improve concrete durability by providing resistance to F/T cycles. An air entrainer admixture is often used to develop the air content system in fresh, high-strength concrete. This study utilized GCP Applied Technologies' Daravair® 1400, an air entrainer with a high-grade saponified rosin formulation similar to Vinsol-based products but with increased purity (GRACE, 2007b). Although the product data sheet indicated no standard addition rate for this air entrainment, typical addition rates range from 0.5 to 3 fl oz/cwt of cement.

3.2.3 Accelerator

This study used solid-grained calcium chloride (77% concentration) as an accelerator. This additive was essential for obtaining HESC because it increases the hydration rate, which increases the early-age strength of the concrete.

3.3 Cement

CEM III was used in this project to obtain high early-strength concrete. The only difference in chemical composition between Type I cement and CEM III is that CEM III typically contains smaller grains, making it finer than Type 1. Mechanistically, the small grains in CEM III cause rapid formation of the hydration products, resulting in quick setting times and strength gain. Table 3-5 shows the data sheet for the Ash Grove cement used in this research.

Table 3-5: CEM III Chemical and Physical Properties

Property		Spec. Limit	Result
Physical Properties			
Blaine fineness, specific surface – Air Permeability (m2/kg)		-	706
Time of Setting, Vicat:	Initial (minutes)	45-375	80
Air Content of Mortar (volume %)		12 max	8
Autoclave Expansion (%)		0.80 max	-0.01
Compressive Strength (psi)	1 Day	1740 min	4167
	3 Days	3480 min	4793
	7 Days	-	5737
Mortar Bar Expansion		-	0.013
Chemical Properties			
SiO2 – Silicon Dioxide (%)		-	20.6
Fe2O3 – Ferric Oxide (%)		-	3
Al2O3 – Aluminum Oxide (%)		-	4.1
CaO – Calcium Oxide (%)		-	62.6
MgO – Magnesium Oxide (%)		6.0 max	2.3
SO3 – Sulphur Trioxide (%)		3.5 max	3.8
Loss on Ignition (%)		3.0 max	2.2
Insoluble Residue (%)		1.5 max	0.49
Na2O – Sodium Oxide (%)		-	0.13
K2O – Potassium Oxide (%)		-	0.52
Equivalent Alkalies (%)		0.6	0.47
Potential Calculated Compounds			
C3S – Tricalcium Silicate (%)		-	53
C2S – Dicalcium Silicate (%)		-	20
C3A – Tricalcium aluminate (%)		-	6
C4AF – Tetracalcium aluminoferrite (%)		-	9

Chapter 4 - Methodology

This chapter describes the methodology for mixing and selecting the proper doses of admixtures. The chapter also contains mix designs, standards, and tests used in this study.

4.1 Ingredient Selection and Proportions

Previous research investigated HESC durability using various CEM III contents and chemical admixtures with a w/c of 0.37 (Porras et al., 2020). Results showed that low cement content improves F/T performance of concrete (Henkensiefken et al., 2011). This current research utilized low (564 lb/yd^3) and high (752 lb/yd^3) cement contents from Porras et al.(2020) to assess IC as it was applied to concrete with LWA, concrete with CCA, and a control mixture containing only virgin fine aggregate. Table 4-1 shows the matrix of mixtures used in this study.

Table 4-1: Matrix of Mixtures

Cement Content	Batch		
Low cement content 564 lb/yd^3	LWA-LC	CCA-LC	Control-LC
High cement content 752 lb/yd^3	LWA-HC	CCA-HC	Control-HC

This research utilized CEM III with a w/c of 0.37 and fine and coarse aggregates in equal quantities (by volume). Chemical admixtures were also used, including a water reducer, air entrainer, and calcium chloride as an accelerator. Although each mixture required different amounts of water reducer and air-entraining agents, they each contained 2% calcium chloride (by cement weight) as an accelerator. To prevent self-desiccation of the cement paste and proportionate with the cement factor, chemical shrinkage factor, and other factors, fine aggregates

were replaced with dried LWA or CCA based on the required amount of stored free water within the LWA or CCA.

4.2 Replacement

The main goal of IC replacement is to provide an appropriate amount of water to react with unhydrated cement to substitute for chemical shrinkage, or self-desiccation. As described in section 2.5.1, Bentz & Snyder (1999) developed equation (1) to determine the required amount of replacement by volume. The chemical shrinkage factor, which is needed for equation (1), can be calculated using ASTM C1608 (2017b), but this study used the value given by the cement supplier (Ash Grove Cement, Inc).

4.3 Small-Trial Mixtures

Small laboratory trials were used to select proper doses of water reducer and air entraining to achieve slump less than 5 inches and air content of 6.5 ± 1.5%, respectively, as listed in KDOT-Section 401 (a), (g) (KDOT, 2015c). The mixing procedures were not as exact as specified in ASTM C192 (2018c) because the materials, especially the cement and pre-wetted aggregates, were very fine, which required extended mixing procedures and high doses of chemical admixtures. Consequently, the mixing process was extended to 3 minutes of mixing, 2 minutes of rest, and then 5 minutes of mixing. The increased final mixing period helped develop the air void system (Zhang & Wang, 2005).

The air-entraining agent was initially mixed with the aggregates and 75% water for 2 minutes prior to adding the cement, at which point timing for the 10-minute mixing cycle began. Water reducer was added 1.5 minutes after the cement was added, and then the water reducer, calcium chloride, and rest of the water were added 1 minute after the addition of the water reducer;

mixing continued until the 3-minute limit of mixing was reached. After a 2-minute rest, mixing continued for another 5 minutes.

The absolute volume method developed by ACI was adopted to calculate the ingredients needed for each mixture. In this method, the aggregates, cement, and water comprise 1 yd^3; air content is also considered. After specifying the cement and water content, the rest volume was divided inti fine and coarse aggregates based on each one's intended percentage in the mix. Specific gravity for each ingredient was essential for converting the volumes into masses. In addition, utilization of a slump test to measure workability and a Super Air Meter (SAM) to measure air content were necessary to control and calibrate the trial mixtures.

4.3.1 Slump Test

A slump test was conducted on each trial mixture according to ASTM C143 (2015c). First, fresh concrete was placed in three layers of equal volume in a damp Abrams cone that was clamped to a flat base. Each layer was rodded 25 times, ensuring that the rod penetrated each layer below. Then the cone was lifted, and the vertical difference between the top of the cone and the center of the top surface of the displaced fresh concrete was recorded to the nearest 0.25 inch. Figure 4-1 shows slump test equipment.

Figure 4-1: Slump Test Apparatus

4.3.2 Air Content

The air content test was conducted using the pressure method on each trial mix design in accordance with ASTM C231 (2017c). The objective of this method is to find the volume of air content by releasing air from a known volume at a known pressure to a concrete-filled pot and then measuring the pressure needed to fill all the air voids within the concrete. First, three layers of equal volumes of fresh concrete were placed in a damp air pressure meter pot. Each layer was rodded 25 times, ensuring that the rod penetrated each layer below. After the third, or final, layer, the excess concrete was removed, and the lip around the perimeter of the pot was cleaned to obtain accurate measurements. A super air meter attached to a steel cover was clamped down with the pot, and then a funnel was used to insert water from one of the petcocks until water steadily

streamed from the other petcock; then both petcocks were closed. When no air was left in the chamber, then 14.5 psi pressure was applied to the chamber. Finally, the lever was used to release the stored air into the concrete-filled pot while the pot was hit with a rubber mallet. Readings of the volume of air content were then recorded. Figure 4-2 shows the SAM apparatus. Type B measurement was done using this apparatus rather than SAM measurement.

Figure 4-2: SAM Apparatus

4.4 Full-Batch Mixing

A Mud Hog mixer was used for mixtures with 3 ft^3 concrete, as shown in Figure 4-3. Eighteen cylinders measuring 4 inches by 8 inches (101.6 mm by 203.2 mm) were cast for the compressive test, and six prisms measuring 3 inches by 4 inches by 16 inches (76.2 mm by 101.6

mm by 304.8 mm) were cast for drying shrinkage and F/T tests. Three prisms measuring 3 inches by 4 inches by 16 inches (76.2 mm by 101.6 mm by 304.8 mm) were later cast for the autogenous shrinkage test. The quantities for each mixture are listed in Table 4-2.

Figure 4-3: Mud Hog Mixer

Table 4-2: Concrete Mix Designs

Constituent	Low Cement Content			High Cement Content		
	LWA-LC	CCA-LC	Control-LC	LWA-HC	CCA-HC	Control-HC
Cement (lb)	564	564	564	752	752	752
Water (lb)	209	209	209	278	278	278
Fine agg. (lb) (SSD)	1214	1057	1536	939	730	1369
Coarse agg. (lb) (SSD)	1510	1510	1510	1346	1346	1346
AEA (fl.oz)	35	64	27	93	50	58
WR (fl.oz)	101	133	107	62	116	80
Calcium Chloride (lb)	13.5	13.5	13.5	18	18	18
Pre-wetted LWA (lb) (SSD)	196.7	----	----	262.3	----	----
Pre-wetted CCA (lb) (SSD)	----	384.5	----	----	512.7	----
Free water (lb)	42.3	42.3	----	56.4	56.4	----
Slump (inch)	2	2.25	2.5	3.5	2.5	2.25
Air content %	7	6.2	6.7	6	5	7

4.5 Tests and Standards

Concrete strength was evaluated using a compressive strength test, and concrete durability was evaluated using autogenous shrinkage, drying shrinkage, and F/T tests.

4.5.1 Compressive Strength

Concrete strength was assessed according to ASTM C39. Three replicate cylinders measuring 4 inches by 8 inches were prepared for testing. Immediately after casting, specimens were transferred to a moisture room, demolded, and stored until they were tested at specific ages.

4.5.2 Autogenous Shrinkage

ASTM C1698 (2009) describes a standardized experiment to measure autogenous shrinkage for cement pastes and mortars in which concrete is poured into a corrugated polymeric

tube and deformation is assessed periodically. However, if the specimens are sealed, autogenous shrinkage for concrete can also be measured using a steel ring and steel gauges according to ASTM C1581. Many researchers have devised non-standardized ways of measuring autogenous shrinkage in concrete, including sealed prisms (Cusson, 2008; Weiss et al., 1999), cylinders (Craeye & De Schutter, 2008), or large corrugated tubes (Tian & Jensen, 2008). The current study utilized sealed prisms due to the ease of concrete placement, even for low-slump concrete. However, the double-wall ring method also permits the placement of low-slump concrete.

Following the method by Cusson (2008), three prisms measuring 3 inches by 4 inches by 16 inches (76.2 mm by 101.6 mm by 304.8 mm) were placed on steel bases and elevated to be connected with two linear variable differential transformers (LVDTs) at both ends of each prism, as shown in Figure 4-4. The tops of the prisms were sealed with plastic sheets, and neoprene was used at both ends of the prisms to allow expansion at the very early age of hardening. Lubrication oil was applied to the sides of the prisms to allow free movement during shrinkage. Figure 4-5 shows how the prisms were connected and made ready to obtain shrinkage readings.

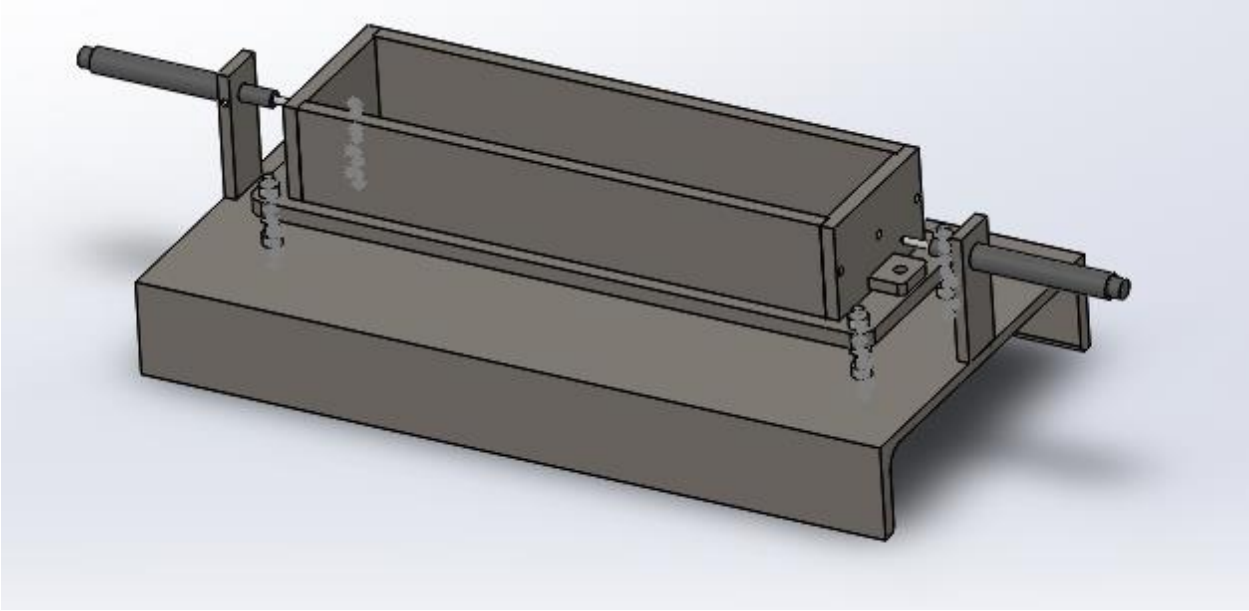

Figure 4-4: Autogenous Shrinkage Apparatus

Figure 4-5: Prisms Measuring Autogenous Shrinkage in Concrete

4.5.3 Drying Shrinkage

Long-term drying shrinkage was evaluated according to ASTM C157. Three prisms measuring 3 inches by 4 inches by 16 inches were cast and covered with a plastic sheet until demolding 6 hours after the moment when water and cement were first mixed. The prisms were then transferred to the moisture room until 24 hours after mixing, at which time they were moved to a container filled with water and calcium hydroxide, where they were left for 14 days to allow complete hydration. Finally, the prisms were transferred to the drying room with 50% RH and 23 ± 2 ^{o}C temperature until the end of experiment. Figure 4-6 shows the length-change comparator apparatus.

Figure 4-6: Length-Change Comparator (ASTM C157)

4.5.4 Freezing and Thawing

This study utilized KTMR-22 to evaluate F/T durability, the focus of this research. Three prisms measuring 3 inches by 4 inches by 16 inches were cast and covered with a plastic sheet until they were demolded 6 hours after the moment when water and cement were first mixed. The prisms were then transferred to the moisture room until they were moved to another treatment regime. KTMR-22 simulates 20 years of harsh environment with 33 cycles per year, requiring 660 cycles instead of 300 cycles. The curing in this study was done in three stages: 1) 67 days in a moisture room at 95% RH at 23 ± 2 ºC, 2) drying in 50% RH at 23 ± 2 ºC until the specimen was 88 days old, and 3) submersion in water at 15.6–26.7 ºC for 24 hours and then submersion in water at 4.4 ºC for another 24 hours. After the 90-day curing period, KTMR-22 follows ASTM C666 procedure (B), in which specimens undergo freezing in cold air and thawing in water. Length change, mass change, and RDME were ˚˚˚measured at intervals less than 56 cycles. The Scientemp F/T machine shown in Figure 4-7 was programmed to automatically run 8 cycles per day. KTMR22 deems the samples nondurable if the RDME drops below 60% or exceeds 0.1% expansion.

Figure 4-7: Scientemp F/T Machine

Chapter 5 - Results

This study obtained slump and air content values for the large batches, as displayed in Table 4-2. The following sections describe the results for each test.

5.1Compressive Strength

Cylindrical molds were demolded 3.5 hours after the cement was mixed with water and then kept in the moisture room until testing. Compressive strength was tested at 4 and 6 hours and 3, 7, 14, and 28 days. An automated variable frequency drive Forney testing machine was used for the compressive strength testing. The specimens were covered by the steel end caps with neoprene pads from both ends to prevent eccentric axial loading, and the ramping rate was 35 ± 7 psi/sec. Figure 5-1 shows the results for the six batches at various ages.

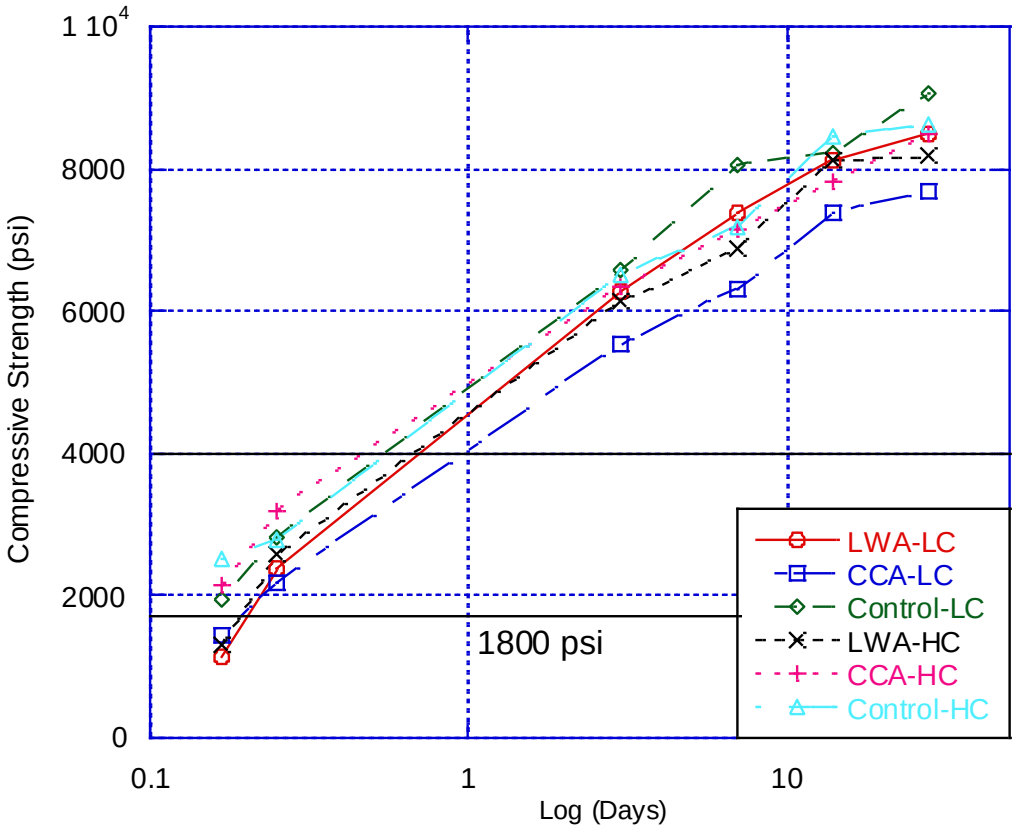

Figure 5-1: Compressive Strength Values for All Batches

5.2 Autogenous Shrinkage

Each experiment for all six concrete batches was run for nine days to ensure steady-state shrinkage development. Data collection started 80 minutes after the water was first mixed with cement to allow time for casting, finishing and sealing, and connecting to the computer. In Figure 5-2, which shows strain development, the positive y-axis represents shrinkage and the negative x-axis represents expansion. Equation (2) was used to calculate autogenous shrinkage measurements.

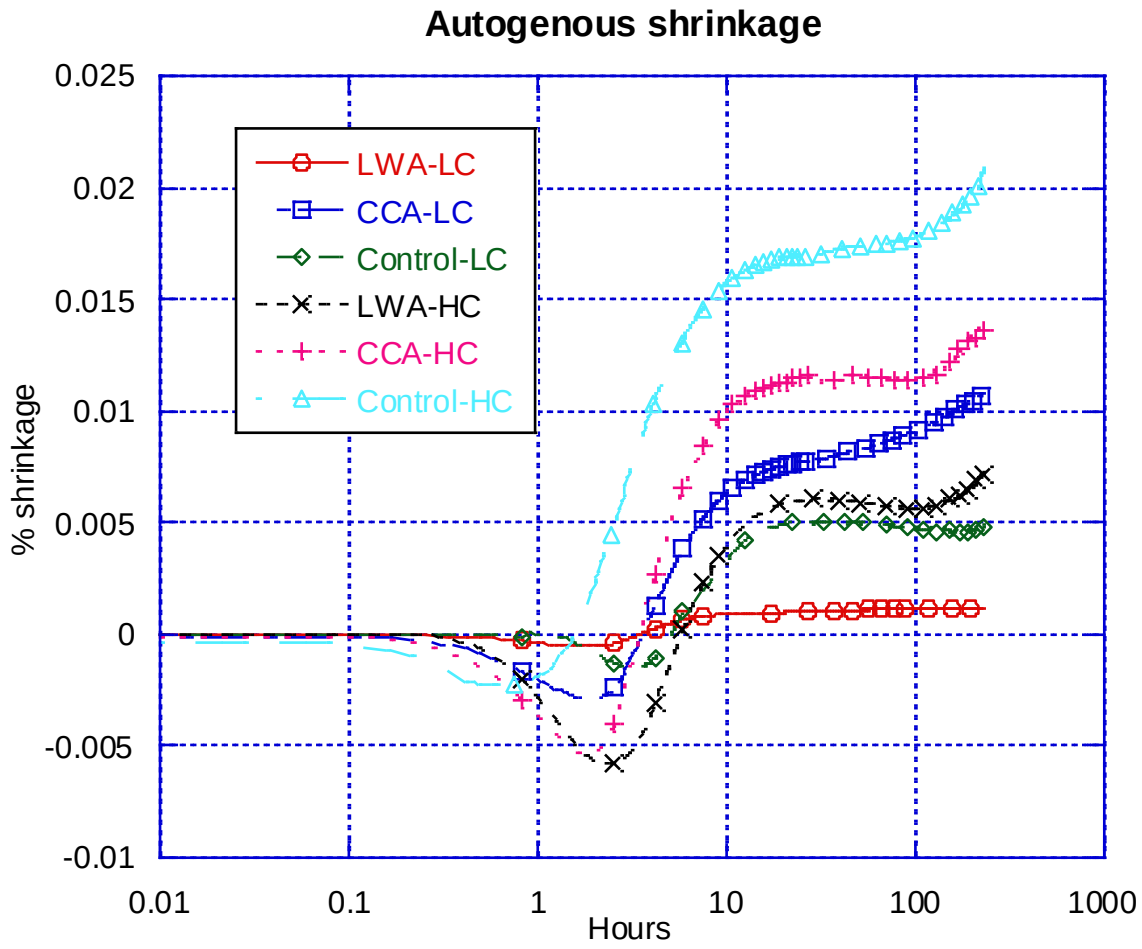

Figure 5-2: Autogenous Shrinkage Measurements for All Batches

$$\Delta Lx = \frac{\pm L}{G} \times 100 \qquad (2)$$

where,

ΔLx = length change of specimen at any age;

$\pm L$ = contraction or expansion of the specimen at any age; and

G = fixed distance between the sawed studs inside the specimen.

5.3 Drying Shrinkage

Figure 5-3 shows drying shrinkage results at 3, 7, 14, and 28 days and 8, 12, 16, and 20 weeks. Equation (3) was used to calculate length change due to drying shrinkage.

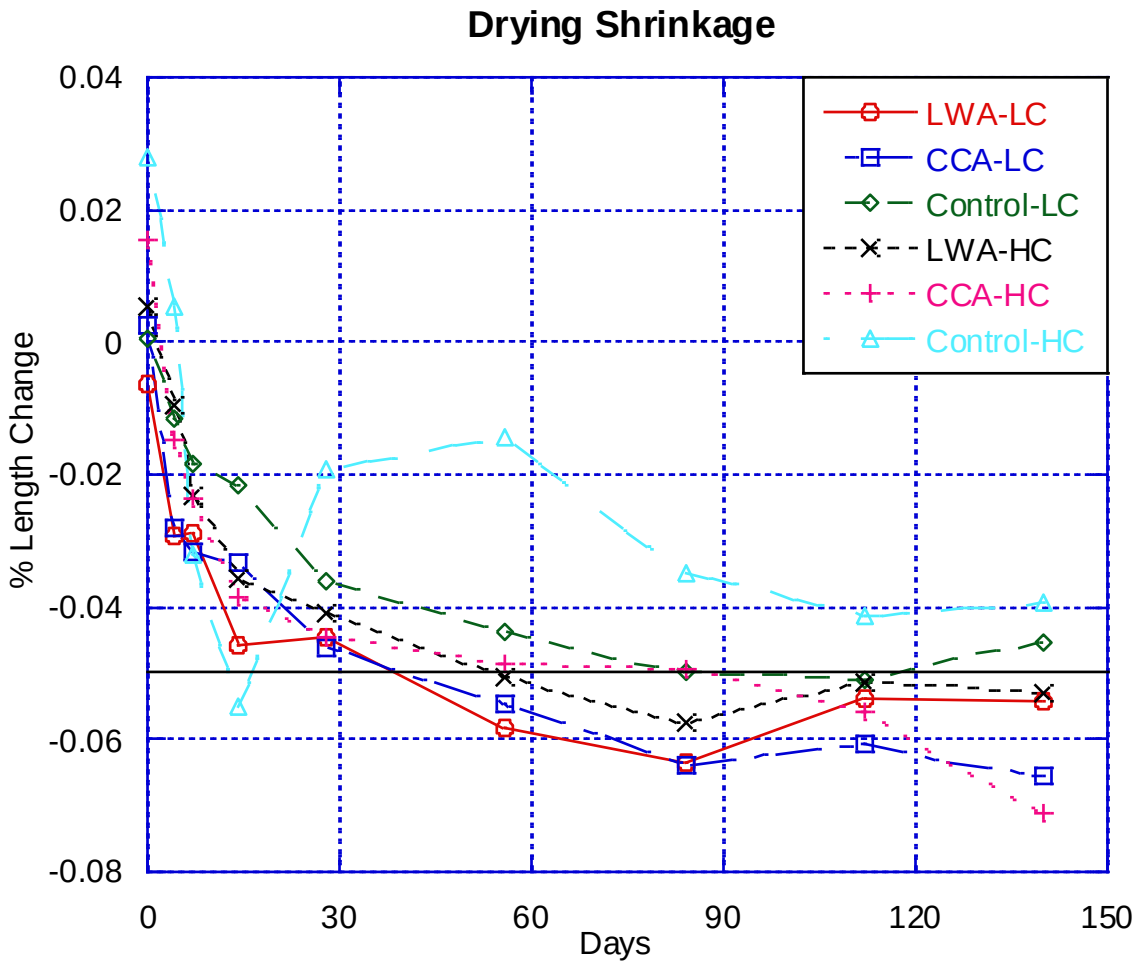

Figure 5-3: Drying Shrinkage Measurements for All Batches

$$\Delta Lx = \frac{CRD - initial\ CRD}{G} \times 100 \qquad (3)$$

where,

ΔLx = length change of specimen at any age %;

CRD = difference between comparator reading of the specimen and the reference bar at any age; and

G = gauge length 16 inches (400 mm).

5.4 Freezing and Thawing

At the end of the 90-day curing period, initial readings were taken for length, mass, and RDME of the samples. Figure 5-4, Figure 5-5, and Figure 5-6 show the time series graphs of these parameters, respectively.

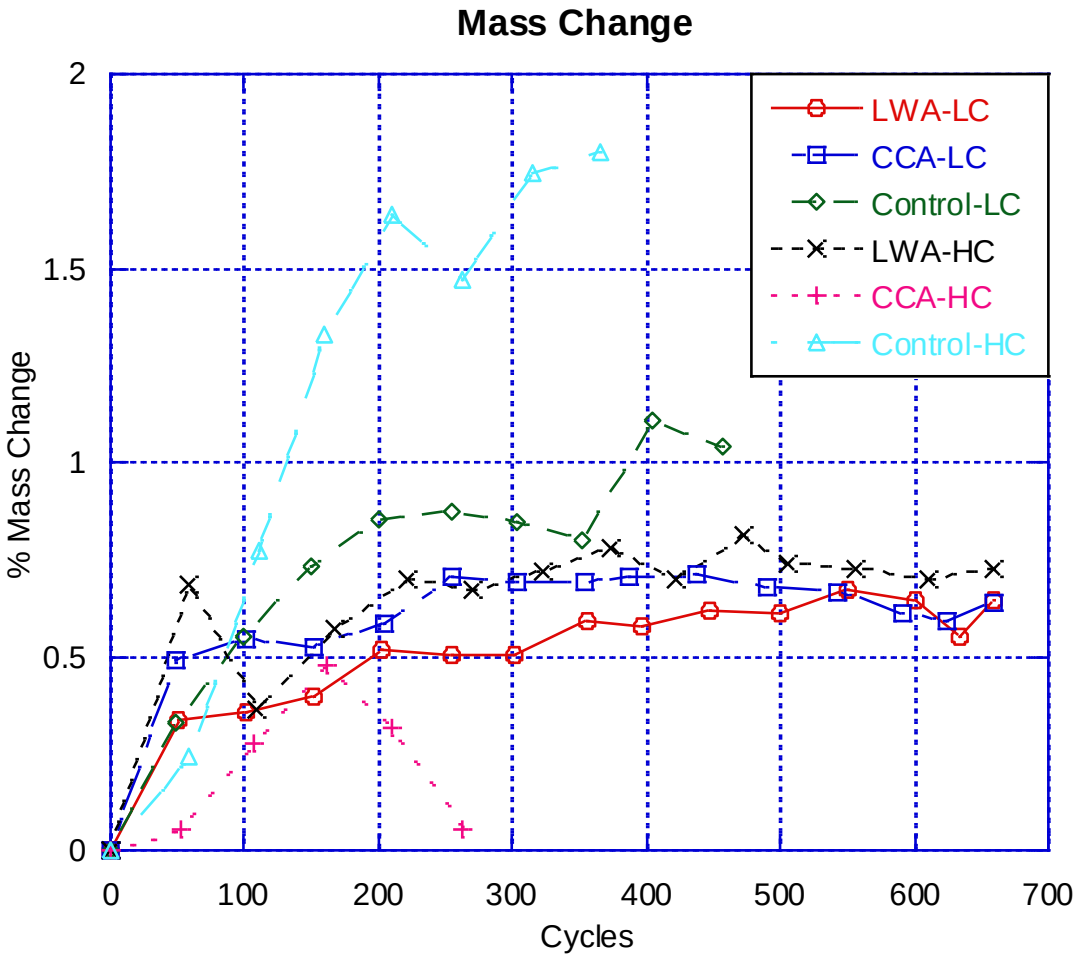

Figure 5-4: Mass-Change Measurements for All Batches

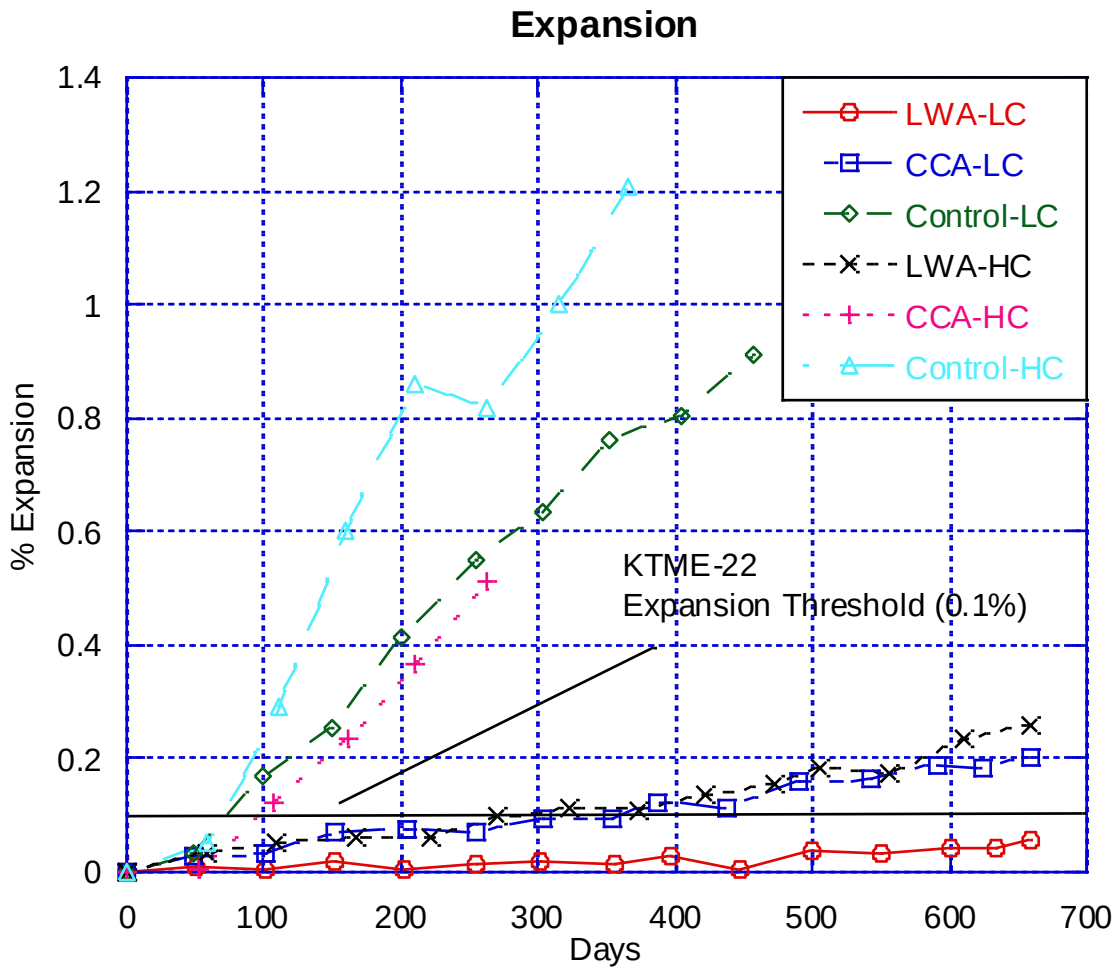

Figure 5-5: Expansion Measurements for All Batches

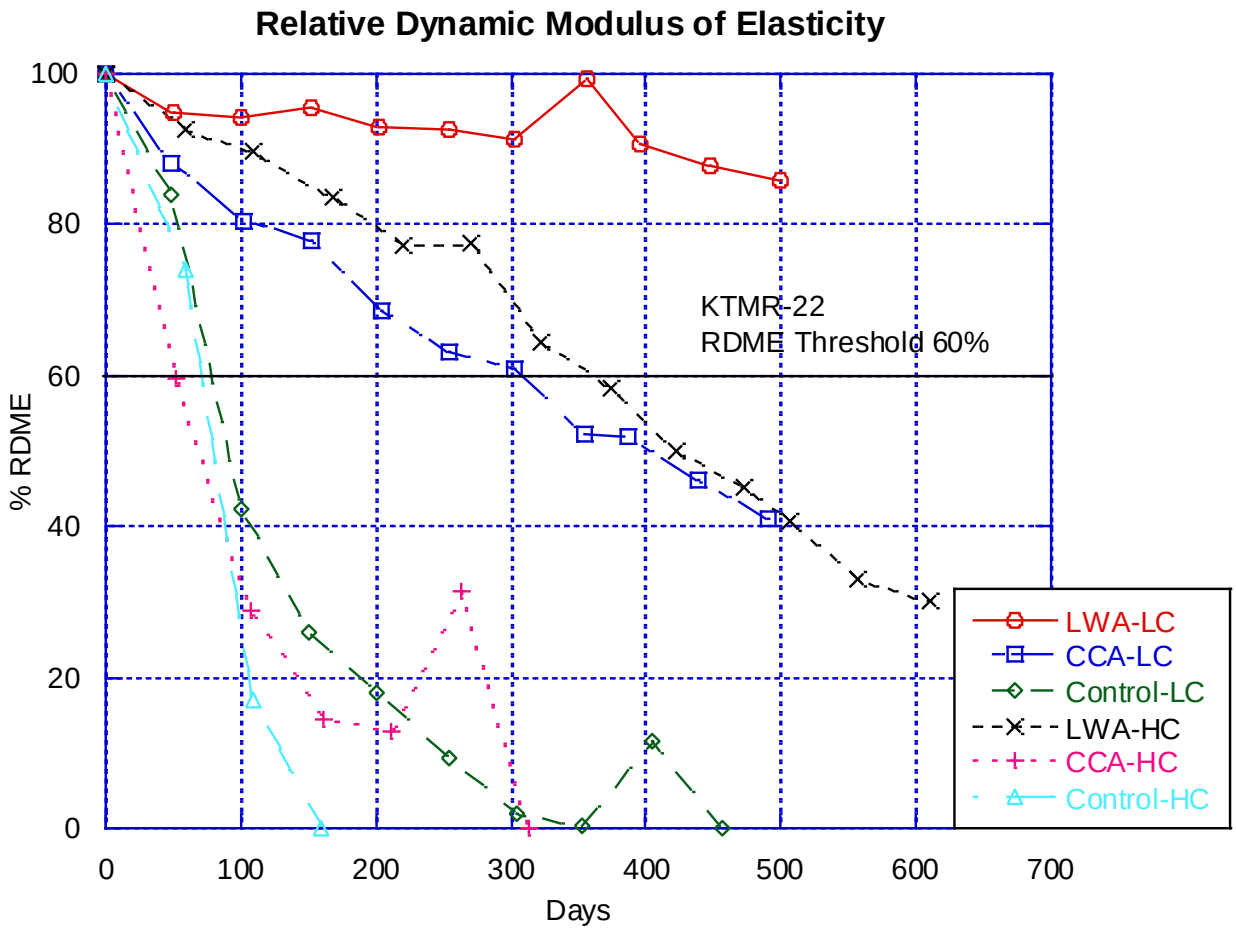

Figure 5-6: RDME Measurements for All Batches

Chapter 6 - Discussion

In Kansas, the compressive strength of HESC must exceed 1,800 psi prior to reopening to traffic. In this study, control-LC, CCA-HC, and control-HC mixtures exceeded the strength requirement at 4 hours, and all other mixtures exceeded 1,800 psi at 6 hours. The low intrinsic strength of LWA, the low localized accelerator dosage due to IC dilution, and the seemingly high localized w/c caused mixtures with LWA to demonstrate decreased early-age strength. The collected strength data indicated that, with the exception of CCA-LC, all mixtures exceeded 8,000 psi at 28 days, indicating that saturated aggregates do not significantly impact the long-term compressive strength for these mixtures.

Autogenous shrinkage measurements accurately predicted shrinkage behavior because shrinkage was first measured after little time from casting the concrete, even though those measurements only reflect the early phase of shrinkage behavior. Meanwhile, a significant amount of data for dry shrinkage measurements was missing because measurements were not initially obtained until 14 days after casting. Drying shrinkage measurements also showed no sensitivity to cracking initiation, which could have caused the fluctuation trend resulting from random cracking. In addition, a standardized threshold for identifying unacceptable drying shrinkage is not available; some state highway agencies use 0.05% as the maximum acceptable value. Therefore, additional measurements besides autogenous shrinkage measurements should be used to accurately quantify concrete performance for drying shrinkage.

The autogenous shrinkage measurements demonstrated the best performance (i.e., lowest shrinkage) for the LWA-LC mixture and the highest shrinkage for the control-HC batch. As expected, batches with low cement contents generally demonstrated lower autogenous shrinkage values than their counterparts with high cement content due to increased internal restraint from

aggregates at lower cement contents. Specifically, LWA-LC showed the lowest value among the low cement content set, followed by control-LC, and then CCA-LC. In the high cement content set, LWA-HC demonstrated the lowest value, followed by CCA-HC and then control-HC, results which contradict the expected trend where control-HC has the highest value, followed by CCA-HC and LWA-HC.

Results from the F/T experiment support the hypothesis that IC improves concrete durability. Mixtures with lowest autogenous shrinkage also demonstrated the best F/T durability. Thus, IC shows promise for HESC durability enhancement. In addition, batches with low cement content showed more F/T durability than batches with high cement content. The content category with optimal F/T performance was LWA, followed by CCA, and then the control batch. Overall, the effectiveness of F/T testing on all batches was revealed in the following order of most to least effective: LWA-LC, LWA-HC, CCA-LC, CCA-HC, control-LC, and control-HC.

KTMR-22 results showed that all batches except the LWA-LC mixture failed prior to passing 660 cycles because the RDME was lower than the 60% threshold or expansion was greater than 0.10%. LWA-LC, CCA-LC, and LWA-HC passed 300 cycles, per ASTM C666 requirements, with RDME greater than 60% and expansion less than 0.10%. The control-HC batch demonstrated the worst performance, failing after approximately 80 cycles.

The IC batches demonstrated increased resistance to F/T cycling possibly due to enhanced hydration of the cement particles associated with IC because of less water penetration into the specimens. Batches LWA-LC, CCA-LC, and LWA-HC had the least mass change, and CCA-HC had the lowest absolute mass change but deteriorated quickly and only survived approximately 260 cycles (Figure 5-4).

Chapter 7 - Conclusion

In this study, IC was evaluated as a potential method to improve the durability of HESC-patching mixtures. The impact of IC on strength, autogenous shrinkage, and F/T durability were specifically evaluated. The following conclusions were drawn from this research:

- The strength gain of internally cured early-age concrete mixtures was less than the control, but the highest strength was very similar for all late-age mixtures. All mixtures met the target compressive strength of 1,800 psi in 6 hours.
- ASTM C157 did not beneficially differentiate the behaviors of the studied HESC mixtures. However, a laboratory-made autogenous shrinkage apparatus reliably measured early-age shrinkage due to chemical shrinkage with sufficient sensitivity to differentiate between mixtures. This apparatus also captured early-age behavior of shrinkage, which is critical for predicting durability.
- The IC technique beneficially mitigates the shrinkage of HESC mixtures, thereby reducing the potential for shrinkage damage.
- As expected, mixtures with high cement content demonstrated greater shrinkage than mixtures with low cement content, as explained by the relatively greater aggregate restraint in low-cement mixtures.
- Concrete mixtures with LWA showed the highest durability based on successful mitigation of autogenous shrinkage and the highest numbers of F/T cycles. From the six batches evaluated, LWA-LC demonstrated the best performance, making it a promising mixture for HESC patching.
- The mixture with the least autogenous shrinkage had the best F/T performance, proving that shrinkage mitigation and F/T resistance are related.

- For optimal IC performance, desorption degree should be adjusted and considerations for plastic; and drying shrinkage should be taken into account, although LWA has the good desorption capability at high RH.
- Because LWA consumes significant energy due to high temperatures needed for liquifying and cooling, CCA could be a more sustainable material if CCA's gradation is adjusted or it is blended with LWA.

References

ACI. (2010). ACI Concrete Terminology. Retrieved from http://www.concrete.org/Technical/CCT/ACI-Terminology.aspx (Jan. 25, 2020).

ACI. (2013). ACI Concrete Terminology. ACI CT-13. American Concrete Institute, Farmington Hills, MI.

Armaghani, J. M., Larsen, T. J., & Romano, D. C. (1992). Aspects of concrete strength and durability. *Transportation Research Record*, 1335.

Asbridge, A. H., Chadbourn, G. A., & Page, C. L. (2001). Effects of metakaolin and the interfacial transition zone on the diffusion of chloride ions through cement mortars. *Cement and Concrete Research*, *31*(11), 1567–1572.

ASCE. (2017). Infrastructure Report Card. Retrieved from https://www.infrastructurereportcard.org/wp-content/uploads/2017/01/Roads-Final.pdf (Jul. 29, 2019).

ASTM. (1997). Standard Test Method for Density, Absorption, and Voids in Hardened Concrete. *ASTM C642-97*, West Conshohocken, PA.

ASTM. (2009). Standard Test Method for Autogenous Strain of Cement Paste and Mortar. *ASTM C1698-09*, West Conshohocken, PA.

ASTM. (2015a). Standard Test Method for Resistance of Concrete to Rapid Freezing and Thawing. *ASTM C666/C666M-15*, West Conshohocken, PA.

ASTM. (2015b). Standard Test Method for Relative Density (Specific Gravity) and Absorption of Fine Aggregate. *ASTM C128-15*, West Conshohocken, PA.

ASTM. (2015c). Standard Test Method for Slump of Hydraulic-Cement Concrete. *ASTM C143-C143-15a*, West Conshohocken, PA.

ASTM. (2017a). Standard Test Method for Length Change of Hardened Hydraulic-Cement Mortar and Concrete. *ASTM C157/C157-17*, West Conshohocken, PA.

ASTM. (2017b). Standard Test Method for Chemical Shrinkage of Hydraulic Cement Paste. *ASTM C1608-17*, West Conshohocken, PA.

ASTM. (2017c). Standard Test Method for Air Content of Freshly Mixed Concrete by the Pressure Method. *ASTM C231-C231-17a*, West Conshohocken, PA.

ASTM. (2018a). Standard Test Method for Compressive Strength of Cylindrical Concrete Specimens. *ASTM C39-C39M-18*, West Conshohocken, PA.

ASTM. (2018b). Standard Test Method for Determining Age at Cracking and Induced Tensile Stress Characteristics of Mortar and Concrete under Restrained Shrinkage. *ASTM C1581 M-18a*, West Conshohocken, PA.

ASTM. (2018c). Standard Practice for Making and Curing Concrete Test Specimens in the Laboratory. *ASTM C192-C192M-18*, West Conshohocken, PA.

ASTM. (2019a). Standard Specification for Rapid Hardening Hydraulic Cement. *ASTM C1600-C1600M-19*, West Conshohocken, PA.

ASTM. (2019b). Standard Test Method for Electrical Indication of Concrete's Ability to Resist Chloride Ion Penetration. *ASTM C1202-19*, West Conshohocken, PA.

ASTM. (2019c). Standard Test Method for Sieve Analysis of Fine and Coarse Aggregates. *ASTM C136-C136-19*, West Conshohocken, PA.

Baghabra Al-Amoudi, O. S., Al-Kutti, W. A., Ahmad, S., & Maslehuddin, M. (2009). Correlation between compressive strength and certain durability indices of plain and blended cement concretes. *Cement and Concrete Composites*, *31*(9), 672–676.

Barcelo, L., Boivin, S., Rigaud, S., Acker, P., Clavaud, B., & Boulay, C. (1999). Linear vs.

volumetric autogenous shrinkage measurement: material behaviour or experimental artifact. *Proceedings of self-dessiccation and its importance in concrete technology*.

Bentz, D., Koenders, E., Monnig, S., Reinhardt, H. W., Van Breugel, K., & Ye, G. (2007). Materials science-based models. *Internal Curing of Concrete*, RILEM Report, *41*, 29–43.

Bentz, D. P., & Snyder, K. A. (1999). Protected paste volume in concrete: Extension to internal curing using saturated lightweight fine aggregate. *Cement and Concrete Research*, *29*(11), 1863–1867.

Bentz, D. P., & Stutzman, P. E. (2008). Internal curing and microstructure of high performance mortars. *ACI SP-256, Internal Curing of High Performance Concretes: Laboratory and Field Experiences*, American Concrete Institute, 81–90.

Bentz, D. P., & Weiss, W. J. (2011). *Internal curing: a 2010 state-of-the-art review*. US Department of Commerce, National Institute of Standards and Technology.

Buenfeld, N. R., & Okundi, E. (1998). Effect of cement content on transport in concrete. *Magazine of Concrete Research*, *50*(4), 339–351.

Castro, J. (2011). Moisture transport in cement-based materials: Application to transport tests and internal curing. Purdue University.

Castro, J., Keiser, L., Golias, M., & Weiss, J. (2011). Absorption and desorption properties of fine lightweight aggregate for application to internally cured concrete mixtures. *Cement and Concrete Composites*, *33*(10), 1001–1008.

Cleary, J., & Delatte, N. (2008). Implementation of internal curing in transportation concrete. *Transportation Research Record*, *2070*(1), 1–7.

Craeye, B., & De Schutter, G. (2008). Experimental evaluation of mitigation of autogenous shrinkage by means of a vertical dilatometer for concrete. *Eight International Conference*

on Creep, Shrinkage and Durability Mechanics of Concrete and Concrete Structures, CRC Press/Balkema, 909–914.

Cusson, D. (2008). Effect of blended cements on effectiveness of internal curing of HPC. *ACI SP-256, Internal Curing of High-Performance Concretes: Laboratory and Field Experiences*, American Concrete Institute, 105–120.

Cusson, D., & Margeson, J. (2010). Development of low-shrinkage high-performance concrete with improved durability. *Sixth International Conference on Concrete under Severe Conditions: Environment and Loading*.

Delagrave, A., Bigas, J. P., Ollivier, J. P., Marchand, J., & Pigeon, M. (1997). Influence of the interfacial zone on the chloride diffusivity of mortars. *Advanced Cement Based Materials*, *5*(3–4), 86–92.

Fakhri, M., Amoosoltani, E., & Aliha, M. R. M. (2017). Crack behavior analysis of roller compacted concrete mixtures containing reclaimed asphalt pavement and crumb rubber. *Engineering Fracture Mechanics*, 180, 43–59.

Friggle, T., & Reeves, D. (2008). Internal curing of concrete paving: laboratory and field experience. *Special Publication*, 256, 71–80.

Gérard, B., & Marchand, J. (2000). Influence of cracking on the diffusion properties of cement-based materials: Part I: Influence of continuous cracks on the steady-state regime. *Cement and Concrete Research*, *30*(1), 37–43.

Golias, M. R. (2010). The use of soy methyl ester-polystyrene sealants and internalcuring to enhance concrete durability. Purdue University.

GRACE. (2007a). ADVA 140M High-range water reducing admixture ASTM C494 Type A and F, and ASTM C1017 Type I. Cambridge, Massachusetts, United States of America.

GRACE. (2007b). DARAVAIR 1400 Air-entraining admixture ASTM C260. Cambridge, Massachusetts, United States of America.

Grassl, P., Wong, H. S., & Buenfeld, N. R. (2010). Influence of aggregate size and volume fraction on shrinkage induced micro-cracking of concrete and mortar. *Cement and Concrete Research*, *40*(1), 85–93.

Guan, Y., Gao, Y., Sun, R., Won, M. C., & Ge, Z. (2017). Experimental study and field application of calcium sulfoaluminate cement for rapid repair of concrete pavements. *Frontiers of Structural and Civil Engineering*, *11*(3), 338–345.

Halamickova, P., Detwiler, R. J., Bentz, D. P., & Garboczi, E. J. (1995). Water permeability and chloride ion diffusion in Portland cement mortars: relationship to sand content and critical pore diameter. *Cement and Concrete Research*, *25*(4), 790–802.

Hearn, N. (1999). Effect of shrinkage and load-induced cracking on water permeability of concrete. *Materials Journal*, *96*(2), 234–241.

Henkensiefken, R., Bentz, D., Nantung, T., & Weiss, J. (2009a). Volume change and cracking in internally cured mixtures made with saturated lightweight aggregate under sealed and unsealed conditions. *Cement and Concrete Composites*, *31*(7), 427–437.

Henkensiefken, R., Briatka, P., Bentz, D., Nantung, T., & Weiss, J. (2010). Plastic shrinkage cracking in internally cured mixtures made with pre-wetted lightweight aggregate. *Concrete International*, *32*(2), 49–54.

Henkensiefken, R., Nantung, T., & Weiss, J. (2009b). Internal curing-from the laboratory to implementation. *International Bridge Conference*.

Henkensiefken, R., Nantung, T., & Weiss, J. (2011). Saturated lightweight aggregate for internal curing in low w/c mixtures: Monitoring water movement using X-ray absorption. *Strain*,

47(1), e432–e441.

Herve, E., & Zaoui, A. (1993). N-layered inclusion-based micromechanical modelling. *International Journal of Engineering Science*, *31*(1), 1–10.

Hornain, H., Marchand, J., Duhot, V., & Moranville-Regourd, M. (1995). Diffusion of chloride ions in limestone filler blended cement pastes and mortars. *Cement and Concrete Research*, *25*(8), 1667–1678.

Jacobsen, S., Marchand, J., & Boisvert, L. (1996). Effect of cracking and healing on chloride transport in OPC concrete. *Cement and Concrete Research*, *26*(6), 869–881.

Jeong, J. -H., & Zollinger, D. G. (2004). Early-age curling and warping behavior: Insights from a fully instrumented test-slab system. *Transportation Research Record: Journal of the Transportation Research Board*, *1896*(1), 66–74.

Justs, J., Wyrzykowski, M., Bajare, D., & Lura, P. (2015). Internal curing by superabsorbent polymers in ultra-high performance concrete. *Cement and Concrete Research*, 76, 82–90.

KDOT. (2012). KT-79: Surface Resistivity Indication of Concrete's Ability to Resist Chloride Ion Penetration. Retrieved from https://www.ksdot.org/Assets/wwwksdotorg/bureaus/burConsMain/Connections/ConstManual/2015/KT-79.pdf (Jul. 29, 2019).

KDOT. (2015a). Section 833 Pavement Patching-Kansas Standard Specifications for State Road & Bridge Construction. Retrieved from https://www.ksdot.org/Assets/wwwksdotorg/bureaus/burConsMain/specprov/2015/833.pdf. (Jul. 29, 2019).

KDOT. (2015b). KTMR-22: Resistance of Concrete to Rapid Freezing and Thawing-Kansas Test Method. Retrieved from

https://www.ksdot.org/Assets/wwwksdotorg/bureaus/burMatrRes/KTMRs/KTMR-22%20(6-27-2018).pdf (Jul. 29, 2019).

KDOT. (2015c). Section 401 General Concrete-Kansas Standard Specifications for State Road & Bridge Construction. Retrieved from https://www.ksdot.org/Assets/wwwksdotorg/bureaus/burConsMain/specprov/2015/401.pdf. (Jul. 29, 2019).

Li, M., & Li, V. C. (2009). Influence of material ductility on performance of concrete repair. *ACI Materials Journal*, *106*(5), 419.

Li, W., Pour-Ghaz, M., Castro, J., & Weiss, J. (2011). Water absorption and critical degree of saturation relating to freeze-thaw damage in concrete pavement joints. *Journal of Materials in Civil Engineering*, *24*(3), 299–307.

Lightweight Aggregate Manufacturing. Retrieved from https://www3.epa.gov/ttn/chief/ap42/ch11/final/c11s20.pdf (Feb. 18, 2020).

Liu, J., Shi, C., Ma, X., Khayat, K. H., Zhang, J., & Wang, D. (2017). An overview on the effect of internal curing on shrinkage of high performance cement-based materials. *Construction and Building Materials*, 146, 702–712.

Lura, P., Pease, B., Mazzotta, G. B., Rajabipour, F., & Weiss, J. (2007). Influence of shrinkage-reducing admixtures on development of plastic shrinkage cracks. *ACI Materials Journal*, *104*(2), 187.

Mindess, S., Young, F. J., & Darwin, D. (2003). *Concrete*. *Technical Documents*, Prentice Hall, NJ.

Philleo, R. (1991). Concrete science and reality. *Materials Science of Concrete*, 1–8.

Porras, Y., Jones, C., & Schmiedeke, N. (2020). Freezing and thawing durability of high early

strength Portland cement concrete. *Journal of Materials in Civil Engineering*, *32*(5), 4020077.

Rao, C., & Darter, M. (2013). Evaluation of internally cured concrete for paving applications. *Applied Research Associates, Inc.*, Champaign, IL.

Ray, G. K. (1980). Effect of defective joint seals on pavement performance. *Transportation Research Record*, 752, 1–2. Retrieved from http://w.sealnoseal.org/PDF/EffectDefect/effect%20of%20defective%20joint%20seals%20on%20pavement%20performance.pdf

Şahmaran Mustafaand Li, V. C. (2009). Influence of microcracking on water absorption and sorptivity of ECC. *Materials and Structures*, *42*(5), 593–603.

Sant, G., Dehadrai, M., Bentz, D., Lura, P., Ferraris, C. F., Bullard, J. W., & Weiss, J. (2009). Detecting the fluid-to-solid transition in cement pastes. *Concrete International*, *31*(6), 53–58.

Saraswathy, V., & Song, H.-W. (2007). Corrosion performance of rice husk ash blended concrete. *Construction and Building Materials*, *21*(8), 1779–1784.

Schlitter, J., Henkensiefken, R., Castro, J., Raoufi, K., Weiss, J., & Nantung, T. (2010). Development of internally cured concrete for increased service life. *Joint Transportation Research Program.*

Shackel, B., & Yamin, S. (1994). Laboratory measurements of water infiltration through concrete block pavements. *Proceedings, 2nd International Workshop on Concrete Block Palving,* Oslo, Norway, 127–133.

Shanahan, N., Bien-Aime, A., Buidens, D., Meagher, T., Sedaghat, A., Riding, K., & Zayed, A. (2016). Combined effect of water reducer–retarder and variable chloride-based accelerator

dosage on rapid repair concrete mixtures for jointed plain concrete pavement. *Journal of Materials in Civil Engineering*, *28*(7), 4016036.

Shekari, A. H., & Razzaghi, M. S. (2011). Influence of nano particles on durability and mechanical properties of high performance concrete. *Procedia Engineering*, 14, 3036–3041.

Shen, D., Wang, X., Cheng, D., Zhang, J., & Jiang, G. (2016). Effect of internal curing with super absorbent polymers on autogenous shrinkage of concrete at early age. *Construction and Building Materials*, 106, 512–522.

Streeter, D. A., Wolfe, W. H., & Vaughn, R. E. (2012). Field performance of internally cured concrete bridge decks in New York state. *Special Publication*, 290, 1–16.

Suraneni, P., Azad, V. J., Isgor, O. B., & Weiss, W. J. (2016). Deicing salts and durability of concrete pavements and joints. *Concr. Int*, *38*(4), 48–54.

Sutter, L., Van Dam, T., Peterson, K. R., & Johnston, D. P. (2006). Long-term effects of magnesium chloride and other concentrated salt solutions on pavement and structural Portland cement concrete. *Transportation Research Record*, *1979*(1), 60–68.

Tian, Q., & Jensen, O. M. (2008). Measuring autogenous strain of concrete with corrugated moulds. *Microstructure Related Durability of cCmentitious Composites*, 1501–1511.

Villarreal, V. H., & Crocker, D. A. (2007). Better pavements through internal hydration. *Concrete International*, *29*(2), 32–36.

Wei, Y. (2008). Modeling of Autogenous Deformation in Cementitious Materials, Restraining Effect from Aggregate, and Moisture Warping in Slabs on Grade. Retrieved from https://deepblue.lib.umich.edu/bitstream/handle/2027.42/61657/yweiz_1.pdf?sequence=1&isAllowed=y

Wei, Y., & Hansen, W. (2008). Pre-soaked lightweight fine aggregates as additives for internal

curing in concrete. *Internal Curing of High-Performance Concretes: Laboratory and Field Experiences*, 35–44.

Weiss, W. J., Abraham, D., & Nantung, T. (2007). SPR 3200—A proposal for a research study on saw-cutting and curing of concrete pavements. *The Joint Transportation Research Program of the Indiana Department of Transportation at Purdue University*, West Lafayette, Indiana, USA.

Weiss, W. J., Borischevsky, B. B., & Shah, S. P. (1999). The influence of a shrinkage reducing admixture on the early-age behavior of high performance concrete. *Fifth International Symposium on the Utilization of High Strength/High Performance Concrete, Sandefjord, Norway*, 1418–1428.

Winslow, D. N., Cohen, M. D., Bentz, D. P., Snyder, K. A., & Garboczi, E. J. (1994). Percolation and pore structure in mortars and concrete. *Cement and Concrete Research*, *24*(1), 25–37.

Witherspoon, P. A., Wang, J. S. Y., Iwai, K., & Gale, J. E. (1980). Validity of cubic law for fluid flow in a deformable rock fracture. *Water Resources Research*, *16*(6), 1016–1024.

Wong, H. S., Buenfeld, N. R., Hill, J., & Harris, A. W. (2007). Mass transport properties of mature wasteform grouts. *Advances in Cement Research*, *19*(1), 35.

Wong, H. S., Zobel, M., Buenfeld, N. R., & Zimmerman, R. W. (2009). Influence of the interfacial transition zone and microcracking on the diffusivity, permeability and sorptivity of cement-based materials after drying. *Mag. Concr. Res*, *61*(8), 571–589.

Wu, Z., Wong, H. S., & Buenfeld, N. R. (2015). Influence of drying-induced microcracking and related size effects on mass transport properties of concrete. *Cement and Concrete Research*, 68, 35–48.

Wu, Z., Wong, H. S., Chen, C., and Buenfeld, N. R. (2019). Anomalous water absorption in cement-based materials caused by drying shrinkage induced microcracks. *Cement and Concrete Research*, 115, 90–104.

Yang, Z., Weiss, W. J., & Olek, J. (2006). Water transport in concrete damaged by tensile loading and freeze–thaw cycling. *Journal of Materials in Civil Engineering*, *18*(3), 424–434.

Zhang, M. H., Tam, C. T., & Leow, M. P. (2003). Effect of water-to-cementitious materials ratio and silica fume on the autogenous shrinkage of concrete. *Cement and Concrete Research*, *33*(10), 1687–1694.

Zhang, S., & Wang, K. (2005). Effects of materials and mixing procedures on air void characteristics of fresh concrete. *Proc. of the 2005 Mid-Continent Transportation Research Symposium*, August, 1–15.